C. P. No. 633

C. P. No. 633

MINISTRY OF AVIATION

AERONAUTICAL RESEARCH COUNCIL

CURRENT PAPERS

Equilibrium Real-Gas Performance Charts for a Hypersonic Shock-Tube Wind-Tunnel employing Nitrogen

By

L. Bernstein, B.Sc. (Eng.), Ph.D.*

LONDON: HER MAJESTY'S STATIONERY OFFICE

1963

SIX SHILLINGS NET

C.P. No.633

Equilibrium Real-Gas Performance Charts for a Hypersonic Shock-Tube Wind-Tunnel employing Nitrogen

- By -
L. Bernstein,* B.Sc.(Eng.), Ph.D.

September, 1961

SUMMARY

Charts are presented covering a wide range of reflected-shock wind-tunnel operating conditions, using nitrogen as the working gas. A statistical-mechanical model of the gas is assumed which takes account of molecular vibration, electronic excitation and dissociation. The gas is assumed to be constantly in equilibrium - that is, the reaction rates are taken to be infinitely fast. The equations of motion are solved with the aid of a digital computer, previously reported results[1] for the state of the shock-processed gas in the shock-tube being used.

CONTENTS

---

1. Introduction

The hypersonic wind-tunnel using a shock-tube to heat and compress the reservoir gas has now become a standard tool in aerodynamic research (see Refs.2,3 for example). The extent to which the reservoir gas is heated is such that, in general the perfect gas laws are no longer applicable. Although many results are available for the performance of the simple shock-tube employing real gases[1,4,5] only limited results have been presented[6,7] for the hypersonic expansion of a real gas in a nozzle. Ref.6 furthermore is only concerned with the performance of the "straight-through" shock-tunnel, now generally accepted to give inadequate testing times, while Ref.7 contains information not directly applicable to shock-tunnels. The present report is concerned with the steady expansion of the shock-processed gas in the reflected-shock tunnel. In many such tunnels a hydrogen driver is used to

generate/

---

*This work was done by Dr. L. Bernstein during the period when he was the holder of a Research Fellowship at the N.P.L.

Replaces A.R.C.23,232.

generate shocks in nitrogen, and nitrogen is assumed to be the working gas here. The test-section conditions are presented in terms of the primary shock Mach number and test section flow Mach number for several initial shock-tube channel pressures. The use of the nozzle area ratio as a parameter has been avoided since the effective value will be uncertain due to boundary-layer growth on the nozzle walls. The equations of motion have been solved with the aid of a Ferranti Mercury digital computer, using an iterative method. The results of Ref.1 for the properties of the gas behind the reflected shock in the shock-tube were used as primary data.

2. Thermodynamic Model of the Gas

The statistical-mechanical model of the gas used in the computations has been described in detail in Ref.1. Only a brief summary is given here, together with the resulting expressions for the thermodynamic properties.

The gas is assumed to be composed of homonuclear diatomic molecules which can absorb energy in translation, electronic excitation, rotation and vibration. The modes are assumed further to be uncoupled, the vibrational energy being that of a simple harmonic oscillator. The rotational characteristic temperature, θ_R, a function of the molecular moment of inertia, is also assumed to be much less than the gas temperature, a condition easily satisfied here (θ_R = 2.88°K for nitrogen). At high temperatures the collisions are sufficiently energetic to produce dissociation of the molecules, and the atoms so produced are assumed capable of absorbing energy in translation and electronic excitation. With these assumptions the following expressions result for the thermodynamic properties (see Notation for the meaning of the symbols).

Specific enthalpy:

$$\frac{H}{R_oT} = \frac{7}{2} + \frac{3}{2}\alpha + \frac{(1-\alpha)\frac{\theta_v}{T}}{e^{\theta_v/T} - 1} + 2\alpha \frac{\sum_0 g_n\left(\frac{\varepsilon_n}{kT}\right)e^{-\varepsilon_n/kT}}{\sum_0 g_n e^{-\varepsilon_n/kT}} + (1-\alpha)\frac{\sum_0 g'_n \frac{\varepsilon'_n}{kT} e^{-\varepsilon'_n/kT}}{\sum_0 g'_n e^{-\varepsilon'_n/kT}} + \alpha\frac{\theta_D}{T} \qquad \ldots(2.1)$$

Specific entropy:

$$\frac{S}{R_o} = \frac{H}{R_oT} + \ell n\, Q_{N_2} + \ell n\left(\frac{1+\alpha}{1-\alpha}\right) \qquad \ldots(2.2)$$

Fractional dissociation by mass:

$$\alpha = \left\{\frac{Kd}{4p + Kd}\right\}^{\frac{1}{2}} \qquad \ldots(2.3)$$

Equilibrium constant:

$$K_d = R_oT\, 2m_o\left(\frac{\pi m_o kT}{h^2}\right)^{\frac{3}{2}}\left(\frac{2\theta_R}{T}\right)\left(1 - e^{-\theta_v/T}\right)\frac{(Q_N^E)^2}{(Q_{N_2}^E)}\, e^{-\theta_D/T} \qquad \ldots(2.4)$$

Specific/

Specific heat at constant pressure:

$$\frac{C_p}{R_o} = \frac{7}{2} + \frac{3}{2}\alpha + \frac{(1-\alpha)\left(\frac{\theta_v}{T}\right)^2 e^{\theta_v/T}}{\left(e^{\theta_v/T} - 1\right)^2} + 2\alpha\left\{\frac{\sum_o g_n\left(\frac{\varepsilon_n}{kT}\right)^2 e^{-\varepsilon_n/kT}}{\sum_o g_n e^{-\varepsilon_n/kT}} - \left[\frac{\sum_o g_n \frac{\varepsilon_n}{kT} e^{-\varepsilon_n/kT}}{\sum_o g_n e^{-\varepsilon_n/kT}}\right]^2\right\}$$

$$+ (1-\alpha)\left\{\frac{\sum_o g'_n\left(\frac{\varepsilon'_n}{kT}\right)^2 e^{-\varepsilon'_n/kT}}{\sum_o g'_n e^{-\varepsilon'_n/kT}} - \left[\frac{\sum_o g'_n \frac{\varepsilon'_n}{kT} e^{-\varepsilon'_n/kT}}{\sum_o g'_n e^{-\varepsilon'_n/kT}}\right]^2\right\}$$

$$+ \frac{\alpha(1-\alpha^2)}{2}\phi^2 \qquad \ldots(2.5)$$

Specific heat at constant volume:

$$\frac{C_v}{R_o} = \frac{C_v}{R_o} - \frac{2}{2-\alpha}\left\{1 + \frac{\alpha(1-\alpha)}{2}\phi\right\}^2 \qquad \ldots(2.6)$$

Low frequency speed of sound:

$$a = \left\{\frac{2R_oT}{2-\alpha}\frac{C_p}{C_v}\right\}^{\frac{1}{2}} \qquad \ldots(2.7)$$

where

$$\phi = \left\{\frac{3}{2} + \frac{\theta_D}{T} - \frac{\frac{\theta_v}{T}}{e^{\theta_v/T} - 1} + 2\left[\frac{\sum_o g_n \frac{\varepsilon_n}{kT} e^{-\varepsilon_n/kT}}{\sum_o g_n e^{-\varepsilon_n/kT}} - \frac{\sum_o g'_n \frac{\varepsilon'_n}{kT} e^{-\varepsilon'_n/kT}}{\sum_o g'_n e^{-\varepsilon'_n/kT}}\right]\right\} \qquad \ldots(2.8)$$

3. Equations of Motion

The equations of motion for the steady isentropic flow of gas through a convergent-divergent nozzle are

$$\rho_w u_w \Delta_w = \rho_* a_* \Delta_* \qquad \ldots(3.1)$$

$$H_5 = H_* + \tfrac{1}{2}a_*^2 = H_w + \tfrac{1}{2}u_w^2 \qquad \ldots(3.2)$$

$$S_5 = S_* = S_w \qquad \ldots(3.3)$$

where the starred quantities are those measured at the nozzle throat, and suffices 5 and w indicate respectively the reservoir and working-section conditions (see Fig.1).

The reservoir conditions H_5 and S_5 are functions of the initial shock-tube conditions, and equations (3.1-3) have been solved for the range of primary shock-wave Mach numbers 3(1)10 for selected channel pressures between 50 and 2000 mm Hg with $T_1 = 290°K$.

The/

The conditions at the nozzle throat are first established by a double iteration procedure, and then the expansion along an isentrope is carried out, the flow conditions being most conveniently established for expansions to selected values of the flow static temperature, T_w. The other flow quantities, p_w, ρ_w, M_w, Δ_w, a_w and R_w are then uniquely determined by equations (2.1-7) and (3.1-3). The viscosity μ_w used in the determination of the Reynolds number R_w, is assumed to be that given by Hirschfelder et al[8], calculated using a Lennard-Jones molecular interaction potential. Since this was only required at selected temperatures T_w, the values of μ_w/μ_1 were fed into the computer as primary data.

A quantity of interest in calibrating the nozzle is the Pitot or impact pressure. In order to calculate this, the equations of motion for the standing normal shock-wave (Fig.1), viz.,

$$\rho_w u_w = \rho_s u_s \qquad \ldots(3.4)$$

$$H_w + \tfrac{1}{2} u_w^2 = H_s + \tfrac{1}{2} u_s^2 \qquad \ldots(3.5)$$

$$p_w + \rho_w u_w^2 = p_s + \rho_s u_s^2 \qquad \ldots(3.6)$$

are first solved in a manner similar to that of Ref.1. The conditions immediately aft of this shock in region s being thus established, the entropy S_s may be calculated. The impact pressure is then determined as that reached as the result of the isentropic deceleration to rest of the gas in region s, so that

$$H_t = H_s + \tfrac{1}{2} u_s^2 = H_s \qquad \ldots(3.7)$$

$$S_t = S_s. \qquad \ldots(3.8)$$

This calculation was also carried out using a double iteration procedure on a digital computer, the stagnation temperature and compressibility being also established. The temperature T_s immediately aft the standing shock was obtained so that a better interpretation of the temperature measured by the Sodium Line reversal[9] technique in this region would be possible. The processes are illustrated qualitatively on a Mollier chart in Fig.2.

The results are presented in Figs.3 - 13. In general ratios are employed referring each quantity to its value in the undisturbed channel gas. The nozzle area ratio is of course referred to the throat area, and the Reynolds number R_1 is defined by

$$R_1 = \frac{\rho_1 a_1}{\mu_1} \text{ per foot}$$

where a_1 is the sound speed in region 1. For $T_1 = 290°K$, assumed throughout these calculations,

$$R_1 = 9400 p_1 \text{ per foot, where } p_1 \text{ is in mm Hg.}$$

4. Discussion of Results

The computations have been carried out for the range of primary shock Mach numbers 3(1)10 and for channel pressures p_1 = 50, 100, 200, 500, 1000 and 2000 mm Hg. However in the form in which they are presented, the results are fairly insensitive to initial channel pressure and consequently only those

for/

for p_1 = 50, 200 and 2000 mm Hg are reproduced. The equilibrium throat temperatures which are of some interest, are shown in Fig.3 for all the channel pressures. T_1 = 290°K was assumed throughout.

A parameter of some interest in connection with the maximum possible running time of a shock-tunnel is the mass flow rate through the nozzle. This is illustrated in Fig.4 where the non-dimensional quantity $\Gamma_{*1} A_{*1} = (\rho_* a_*)/(\rho_1 a_1)$ has been plotted against the primary shock Mach number. In the ideal case in which all the shock-processed gas which was initially in the channel is available for test purposes, the running time would be given by:

$$\delta t = \frac{\Delta_{1*}}{\Gamma_{*1} A_{*1}} \cdot \frac{L}{a_1} \qquad \ldots(4.1)$$

where $\Delta_{1*} = \Delta_1 / \Delta_*$ is the ratio of channel cross-section area to throat area, L is the channel length and a_1 the sound speed in the undisturbed channel gas. However this must be considerably modified because of viscous effects in the channel and wave interactions arising from imperfect tailoring (see for example Refs.2 and 10).

Among the experimental methods used for calibrating a nozzle perhaps the most common is that in which the impact pressure distribution is measured and the flow Mach number inferred from this and the reservoir pressure. The ratio of impact pressure to reservoir pressure is shown in Fig.11 as a function of shock Mach number and test section flow Mach number.

The impact pressure is not very sensitive to departures from equilibrium, but some of the other properties are. The effects of finite reaction rates - that is, of vibrational and chemical relaxation - are beyond the scope of this report. They are discussed in Refs.11 - 14. Until a better knowledge of the relevant reaction rates are available, detailed computations are not justified. The available experimental evidence[12] suggests that for p_1 greater than about 200 mm Hg the flow is likely to be near equilibrium for area ratios up to at least 150 for reservoir temperatures T_5, up to 5000°K.

Stollery[11] has attempted temperature measurements at the stagnation point of a blunt body using the spectrum line reversal method[9]. The actual point of measurement behind the stand-off shock must be uncertain in view of the small distance between the shock and the body. For comparison purposes therefore, the temperatures immediately aft of the shock and those at the stagnation point are shown in Figs.10 and 12. When the reservoir gas has been heated by the reflection of a shock of strength above about $W_{11} = 6$, the kinetic energy remaining in the gas after passing through the stand-off shock is absorbed mainly in dissociating the molecules rather than in raising the gas temperature, especially at large expansion ratios.

5./

5. Notation

A_{ij}	sound speed ratio a_i/a_j
a_i	sound speed in region i
C_p, C_v	specific heats at constant pressure and constant volume respectively
D	dissociation energy - electron volts
g_n	spectroscopic weight terms for atomic species
g'_n	spectroscopic weight terms for molecular species
H_i	specific enthalpy in region i
h	Planck's constant - 6.62517×10^{-27} erg-seconds
K_d	equilibrium constant for dissociation reaction
k	Boltzmann's constant - 1.38044×10^{-16} ergs/°K
L	channel length
M_i	flow Mach number in region i
m_o	atomic weight
N	Avogadro's constant - 6.02322×10^{23} molecules/mole.
p_i	pressure in region i
p_{ij}	pressure ratio p_i/p_j
Q_{N_2}	partition function for molecular species
Q^E_j	electronic partition function for species j
R_o	molecular gas constant - $kN/2m_o$
R_i	Reynolds number in region i
S_i	specific entropy of region i
T_i	temperature of region i
u	gas velocity
W_{11}	primary shock Mach number
α	dissociation fraction by mass
Γ_{ij}	density ratio ρ_i/ρ_j
Δ	cross-section area
ε_n, ε'_n	energy levels above ground state for atoms and molecules respectively
θ_D =	D/k; characteristic dissociation temperature
θ_R	characteristic rotational temperature
θ_v	characteristic vibrational temperature
ρ_i	density of region i
μ_i	dynamic viscosity of region i

Suffices

1 2 3 4 5 8 w t refer to regions so labelled in Fig.1

References/

References

No.	Author(s)	Title, etc.
1	L. Bernstein	Tabulated solutions of the equilibrium gas properties behind the incident and reflected normal shock-wave in a shock-tube. I. Nitrogen. II. Oxygen. Communicated by Prof. A. D. Young. A.R.C. C.P.626, April, 1961.
2	D. W. Holder and D. L. Schultz	On the flow in a reflected-shock tunnel. A.R.C. R. & M.3265, August, 1960.
3	A. Herzberg, H. S. Glick, W. E. Smith and W. Squire	Modifications of the shock tube for the generation of hypersonic flow. C.A.L. Rep. AD-789-A-2, March, 1955.
4	S. Feldman	Hypersonic gas dynamic charts for equilibrium air. AVCO Rep. (No number), January, 1957.
5	E. L. Resler, S. C. Lin and A. Kantrowitz	Production of high-temperature gases in shock-tubes. J.App.Phys. 23 (12) 1390, December, 1952.
6	B. A. Woods	Performance estimates for the R.A.E. 6 in. high-pressure shock-tube. A.R.C.20,440, May, 1958.
7	W. D. Erickson and H. S. Creekmore	A study of equilibrium real-gas effects in hypersonic air nozzles including charts of thermodynamic properties of equilibrium air. N.A.S.A. TN D-231, April, 1960.
8	F. D. Rossini (Ed.)	Thermodynamics and physics of matter. Section D. O.U.P.(London) 1955.
9	J. G. Clouston, A. G. Gaydon and I. R. Hurle	Temperature measurements of shock-waves by spectrum-line reversal; II. A double beam method. Proc. Roy. Soc. A 252 p.143, September, 1959.
10	G. Anderson	Shock-tube testing time. J.Ae.Sci. 26 (3) 184, March, 1959.
11	J. L. Stollery	Stagnation temperature measurements in a hypersonic gun tunnel using the Sodium-line reversal method. Imperial College of Science and Technology. Aeronautics Department Report No.16 A.R.C.22,854, May, 1961.
12	H. T. Nagamatsu, R. E. Geiger and R. E. Sheer, Jr.	Real gas effects in flow over blunt bodies at hypersonic speeds. Gen. Elec. Lab. Rep. No. 59-RL-2177 A.R.C.21,083, June, 1959.
13	K. N. C. Bray	Departure from dissociation equilibrium in a hypersonic nozzle. Communicated by Dr. J. W. Maccoll. A.R.C.19,983, March, 1958.
14	J. L. Stollery and J. E. Smith	A note on the variation of vibrational temperature along a nozzle. A.R.C.22,854 (Addendum), June, 1961.

Table 1/

Table 1

Characteristic Gas Properties Assumed for Computations

Atomic weight;	m_o	14.008
Characteristic rotational temperature;	θ_R	2.8785 °K
Characteristic vibration temperature;	θ_v	3353.4 °K
Characteristic dissociation temperature;	θ_D	113,300°K
Electronic energy levels	ε_o/k	0
	ε_1/k	27,700 °K
	ε_2/k	41,500 °K
	ε_o'/k	0
Statistical weight terms	g_o	4
	g_1	10
	g_2	6
	g_o'	1
Undisturbed gas state	T_1	290 °K
	a_1	347.07 metres/sec

FIG. 1

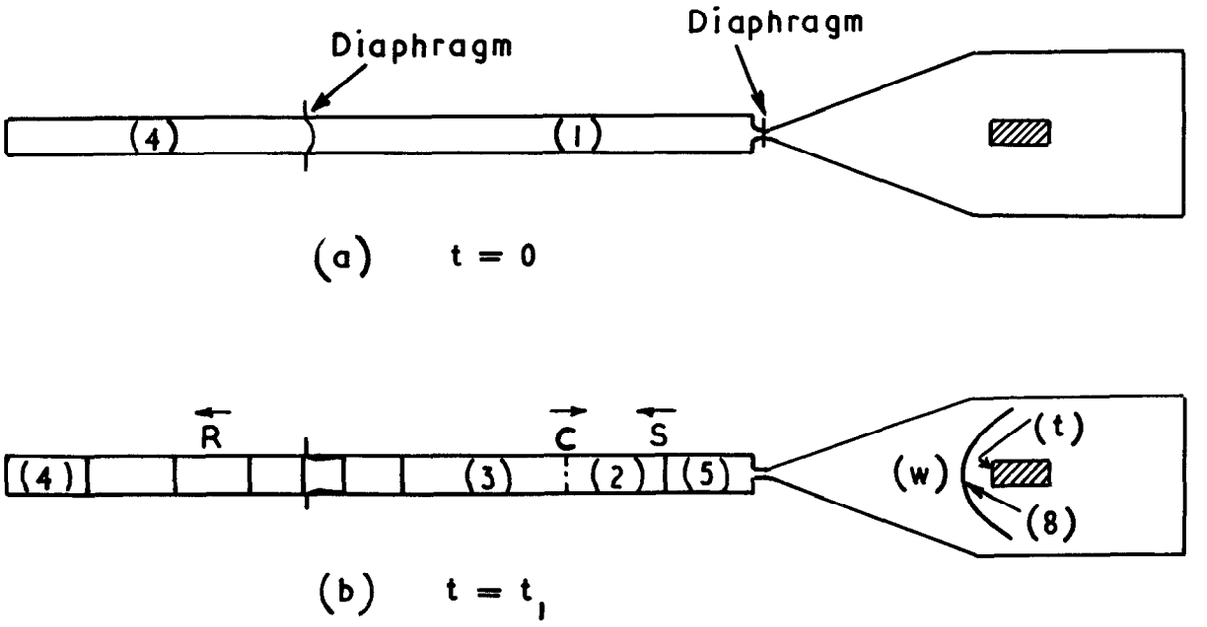

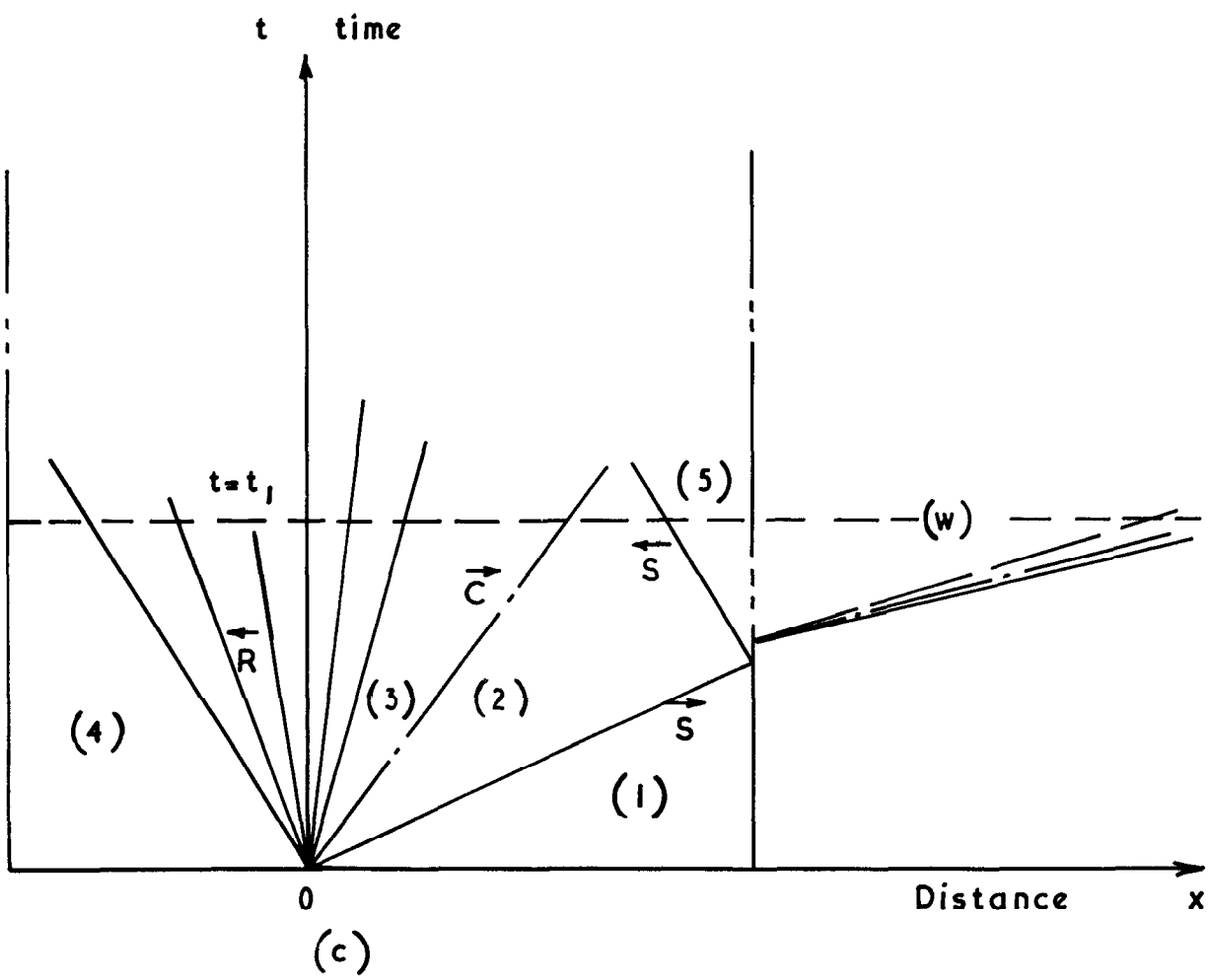

Flow in the hypersonic shock tunnel

(a), (b) Physical plane

(c) Distance - time plane

FIG. 2

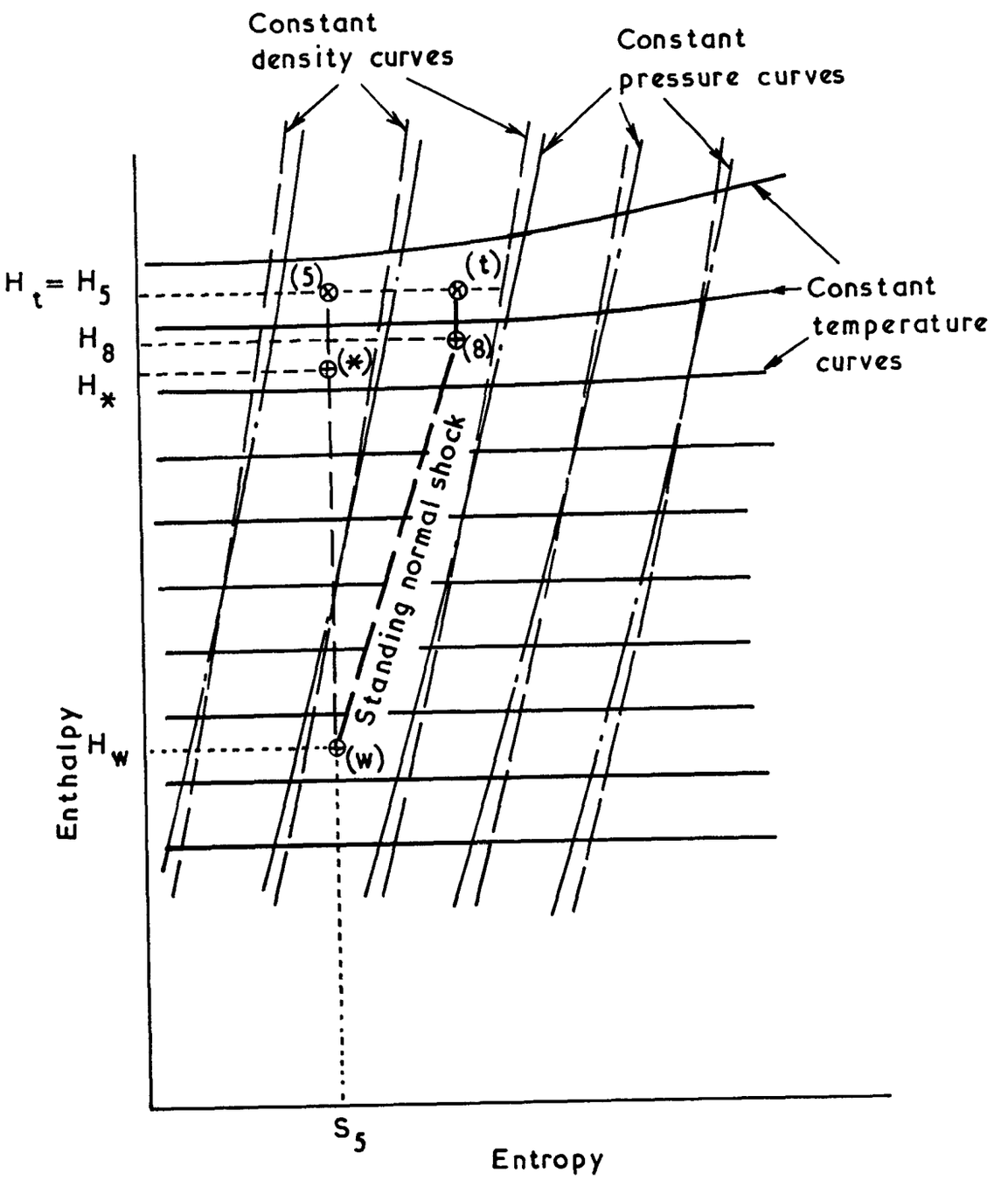

Equilibrium steady expansion and shock compression processes illustrated on Mollier chart.

FIG. 3.

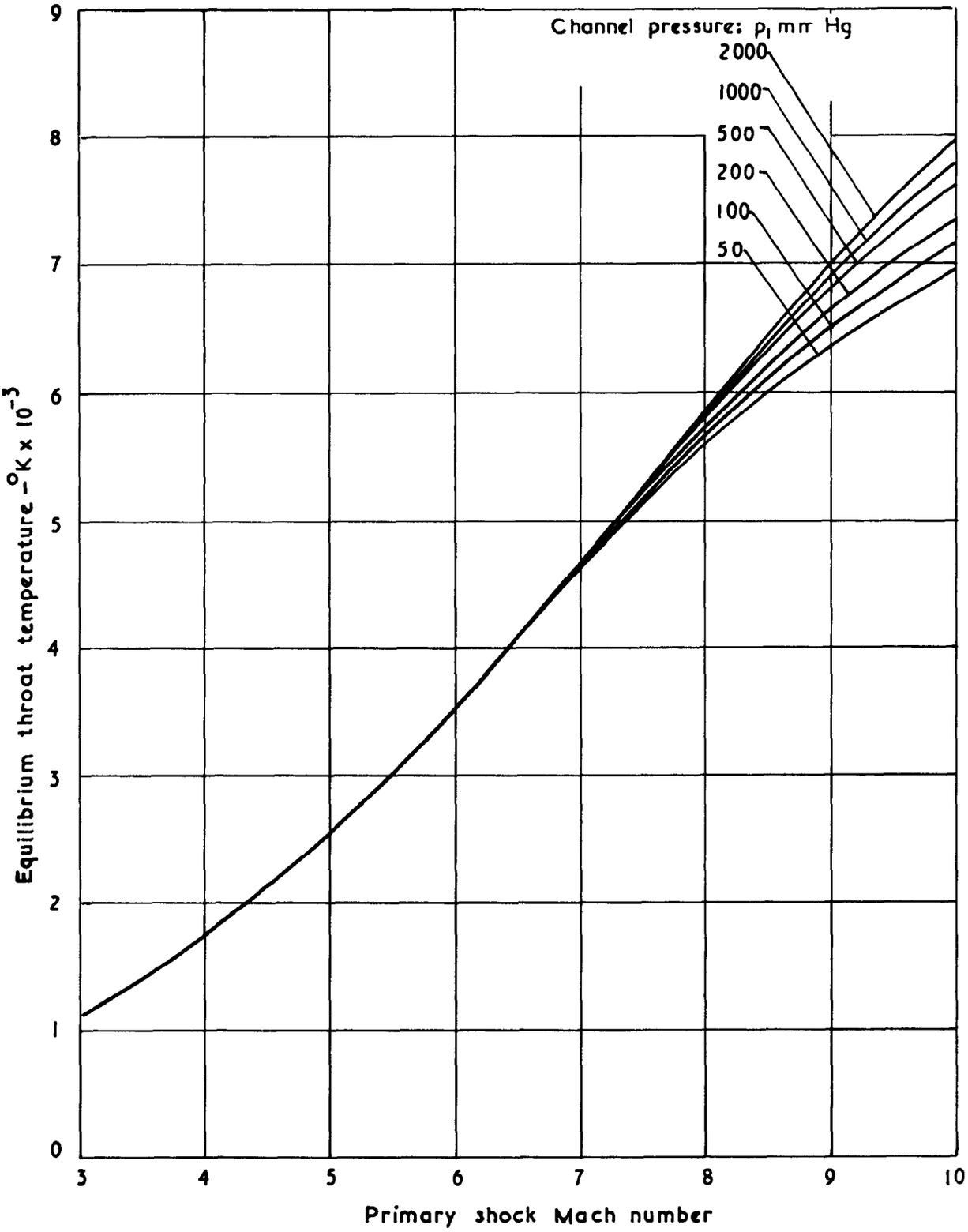

Nozzle throat temperature in reflected shock tunnel.

FIG.4

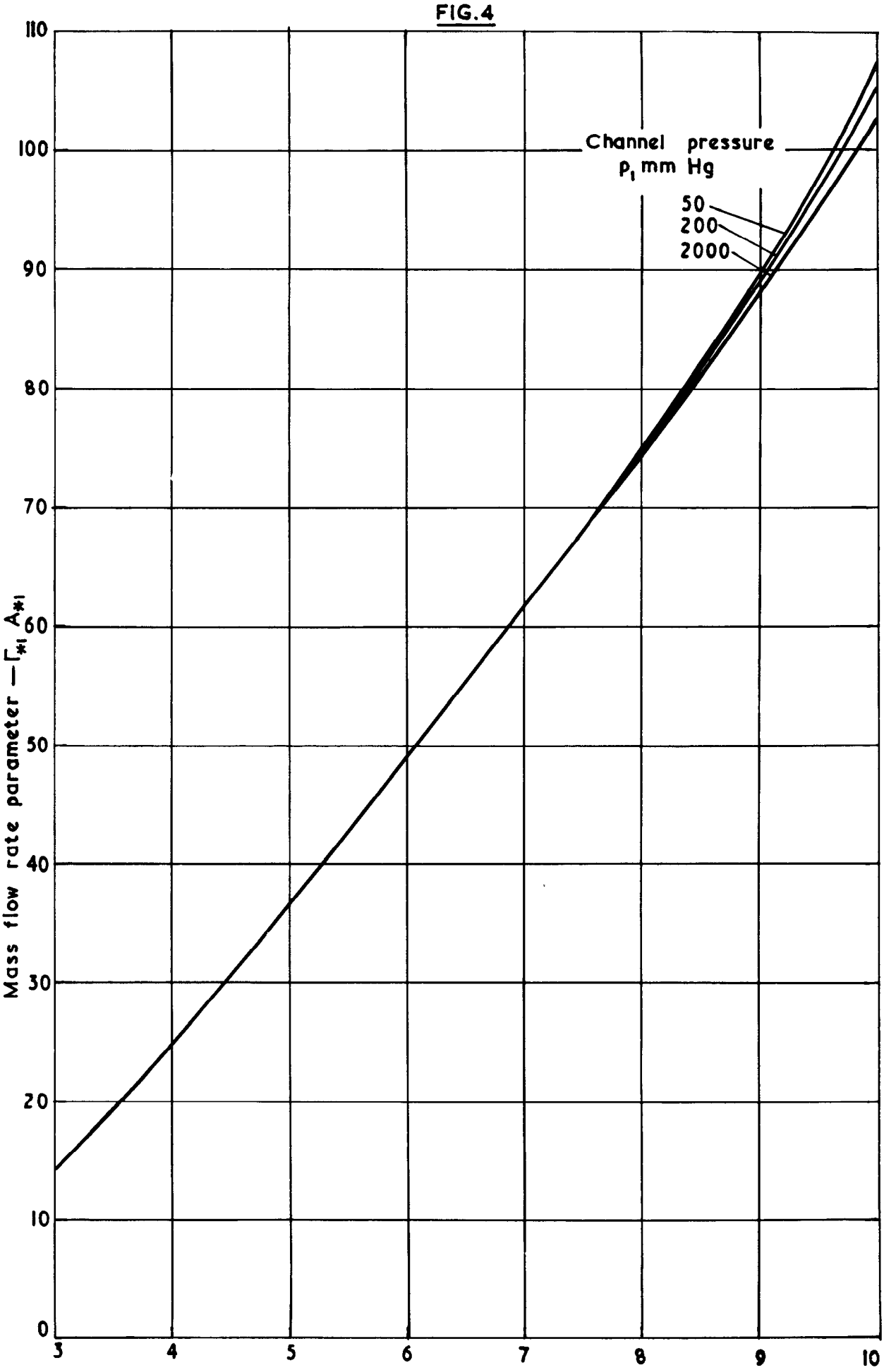

Nozzle mass flow rate parameter.

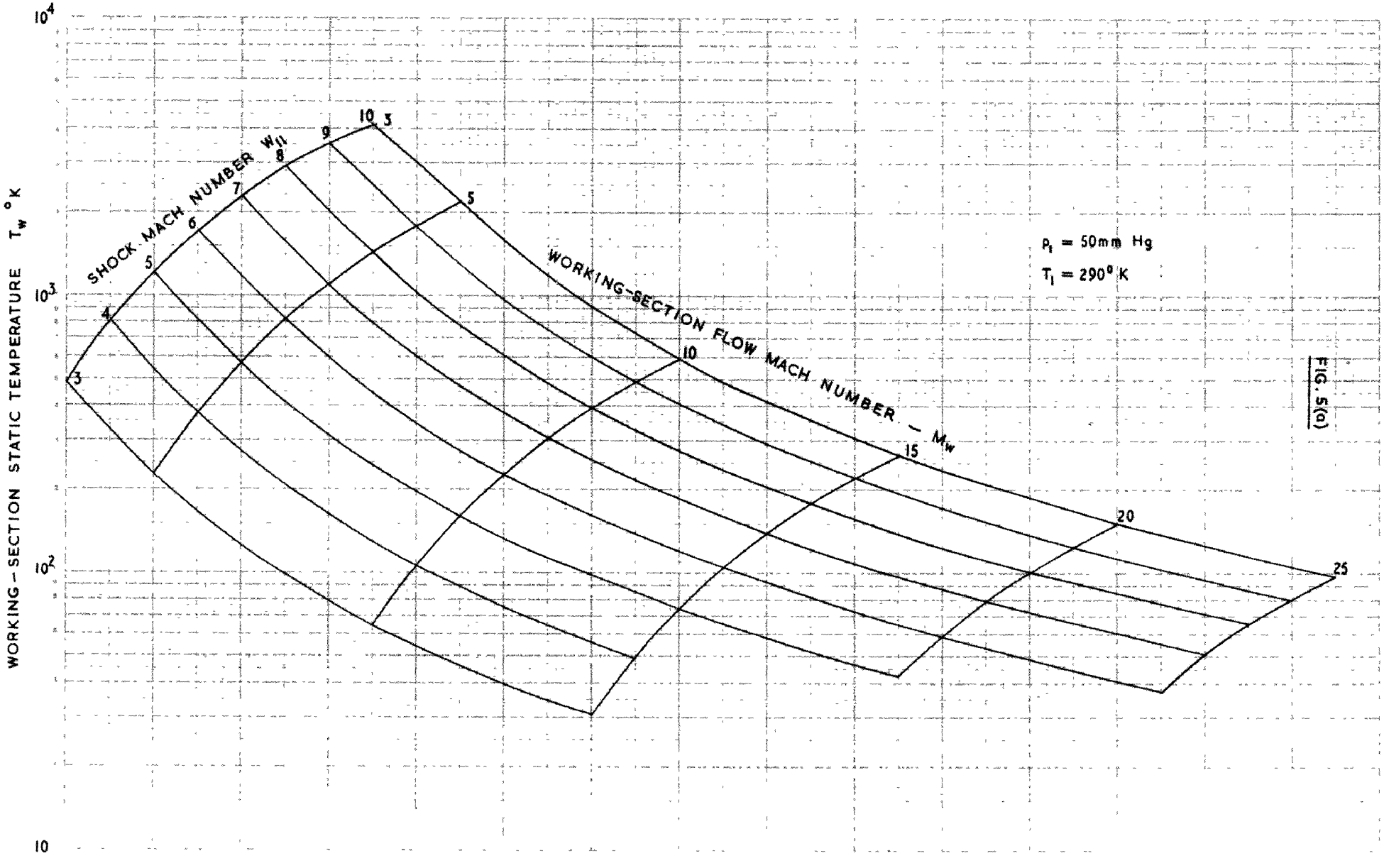

FIG. 5 (a) WORKING-SECTION STATIC TEMPERATURE

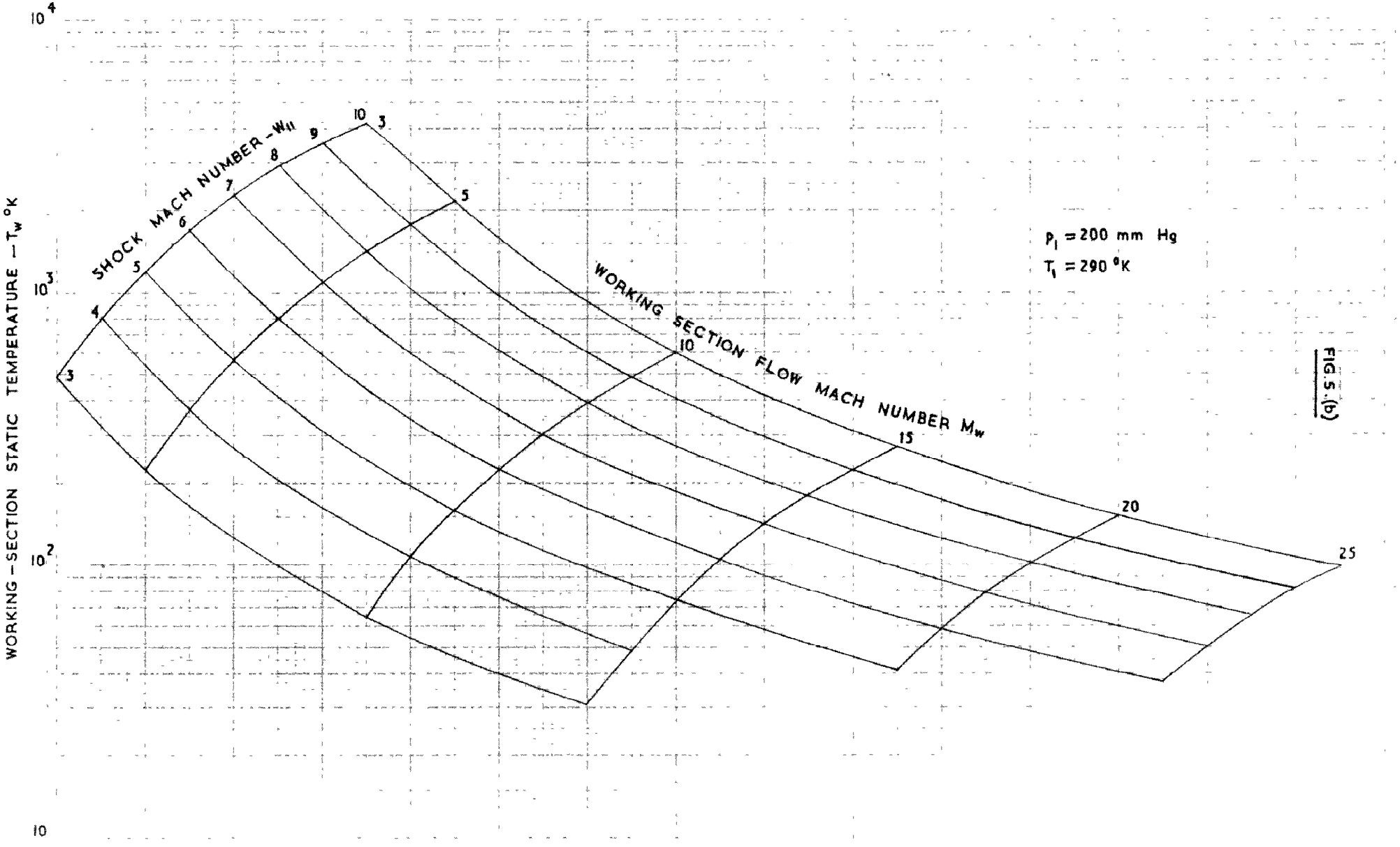

FIG. 5 (b) WORKING – SECTION STATIC TEMPERATURE

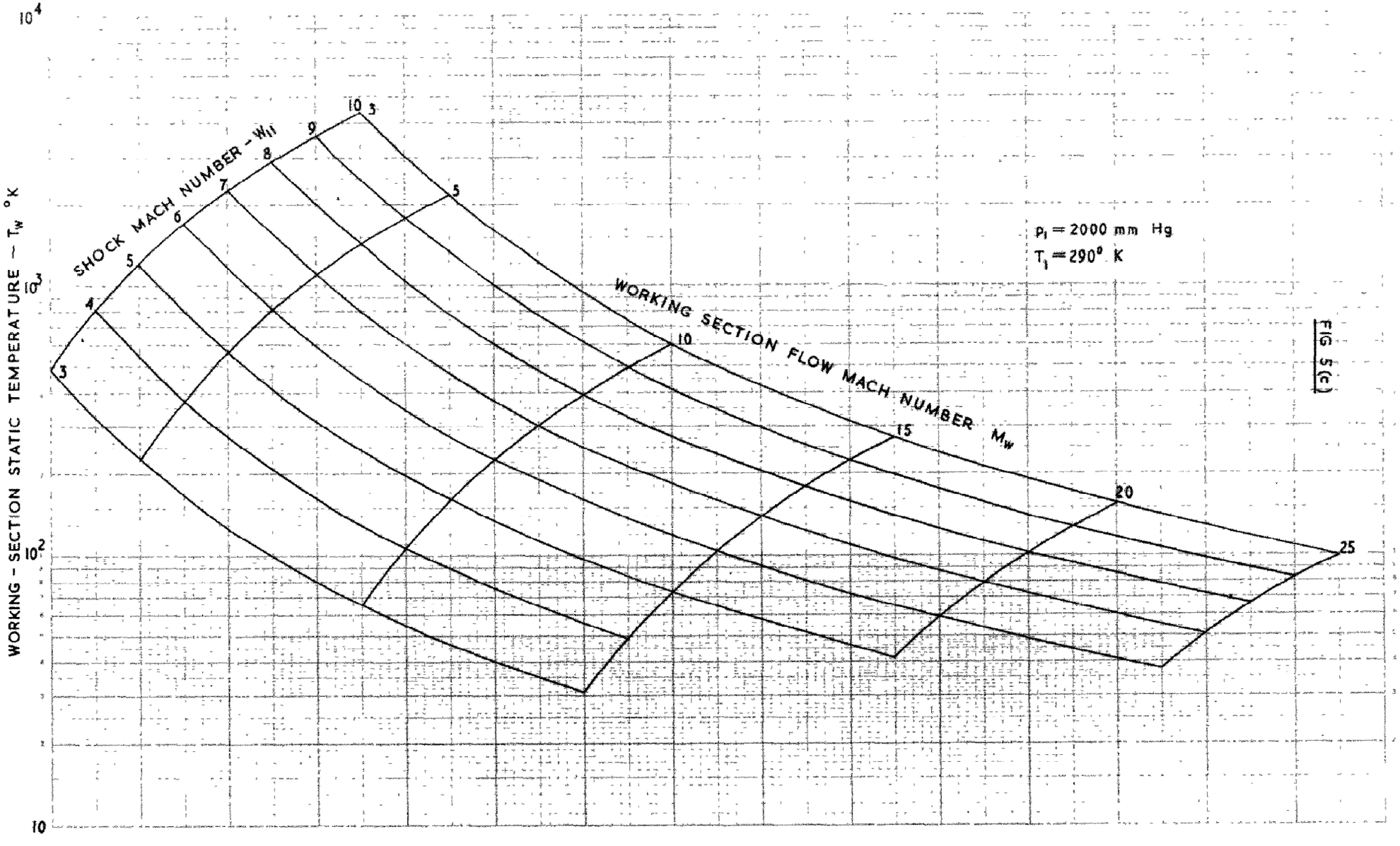

FIG 5(c) WORKING-SECTION STATIC TEMPERATURE

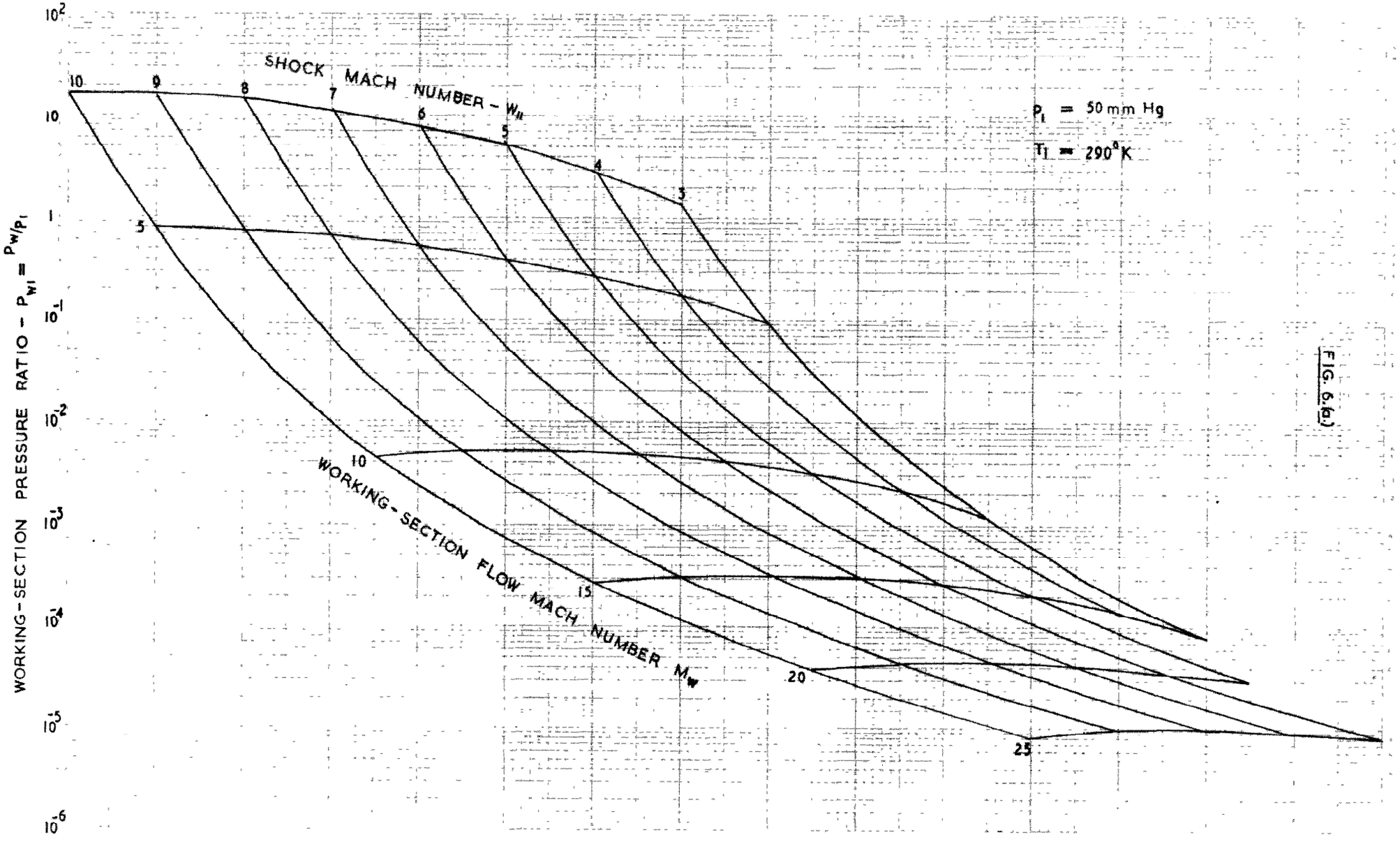

FIG. 6(a) WORKING SECTION STATIC PRESSURE

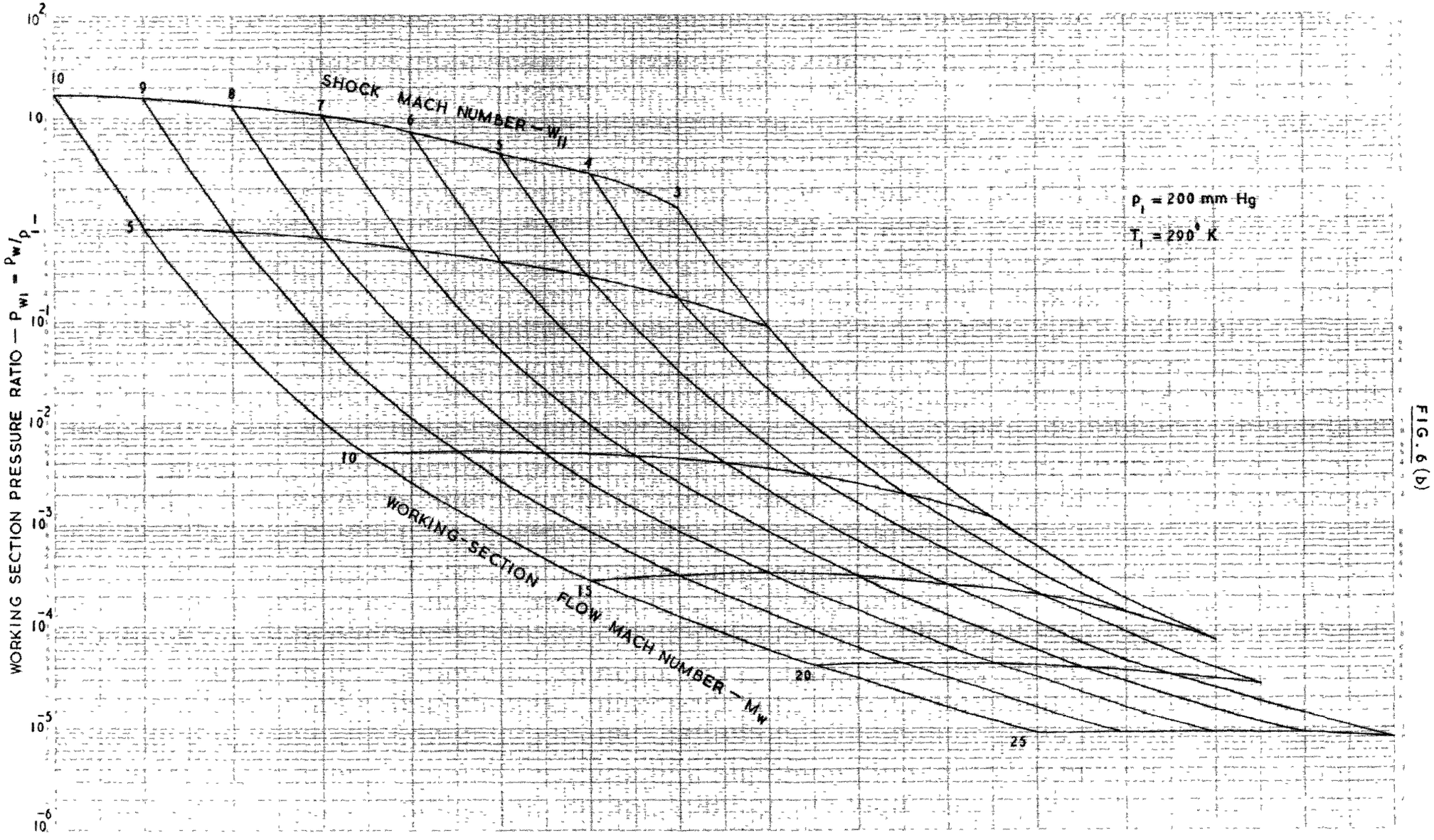

FIG. 6(b) WORKING SECTION STATIC PRESSURE

FIG. 6 (b)

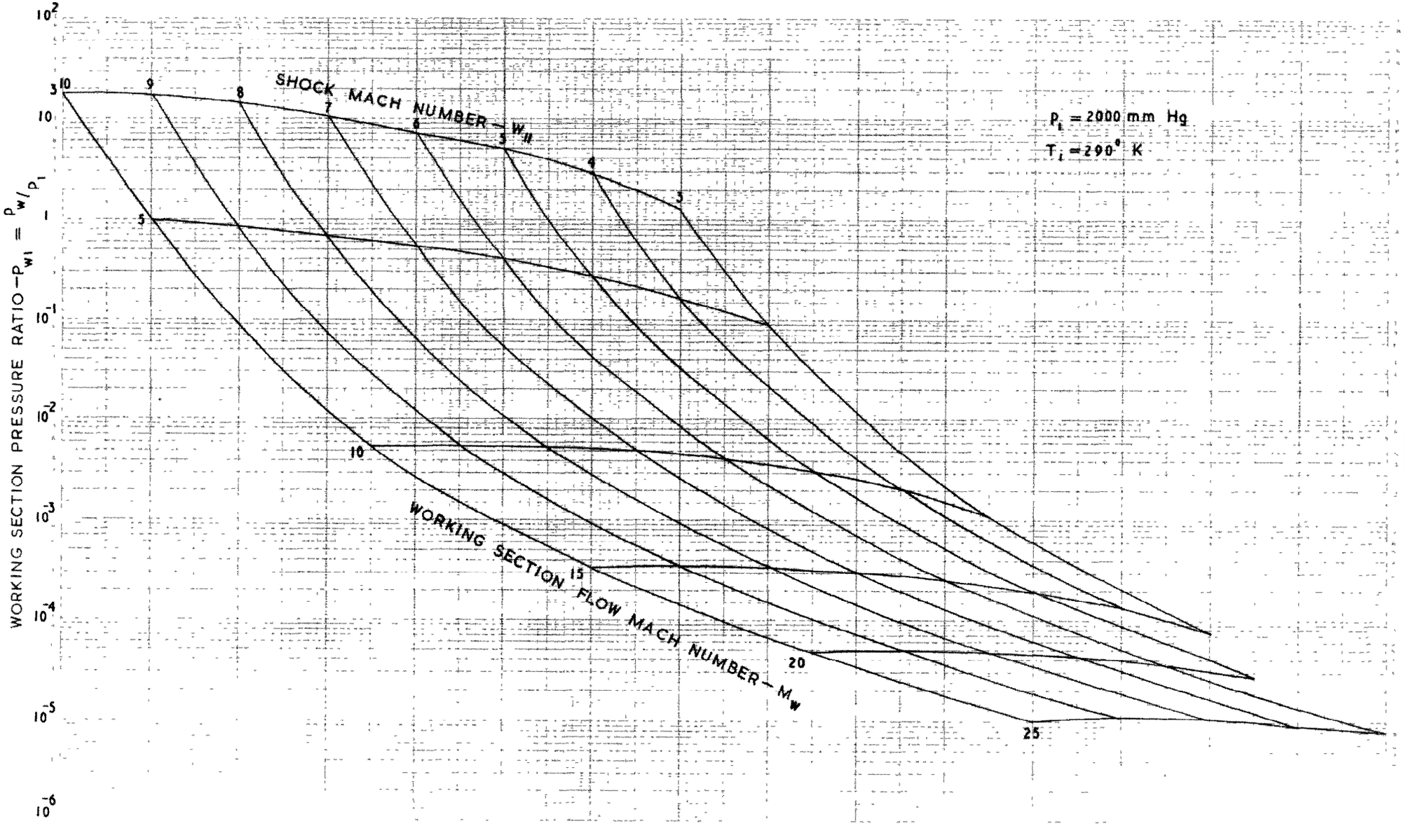

FIG. 6(c)

FIG 6(c) WORKING-SECTION STATIC PRESSURE

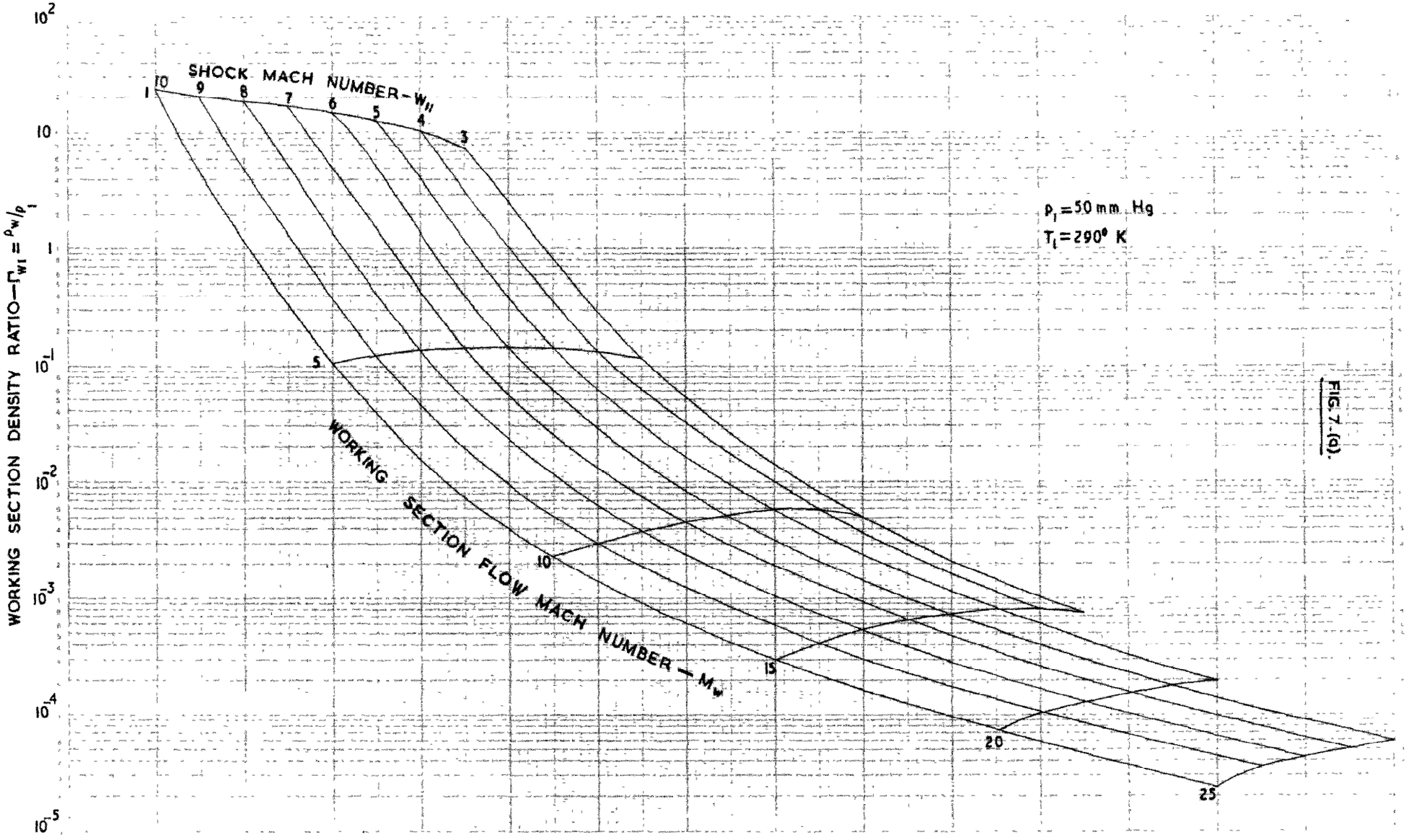

FIG. 7 (a) WORKING – SECTION STATIC DENSITY

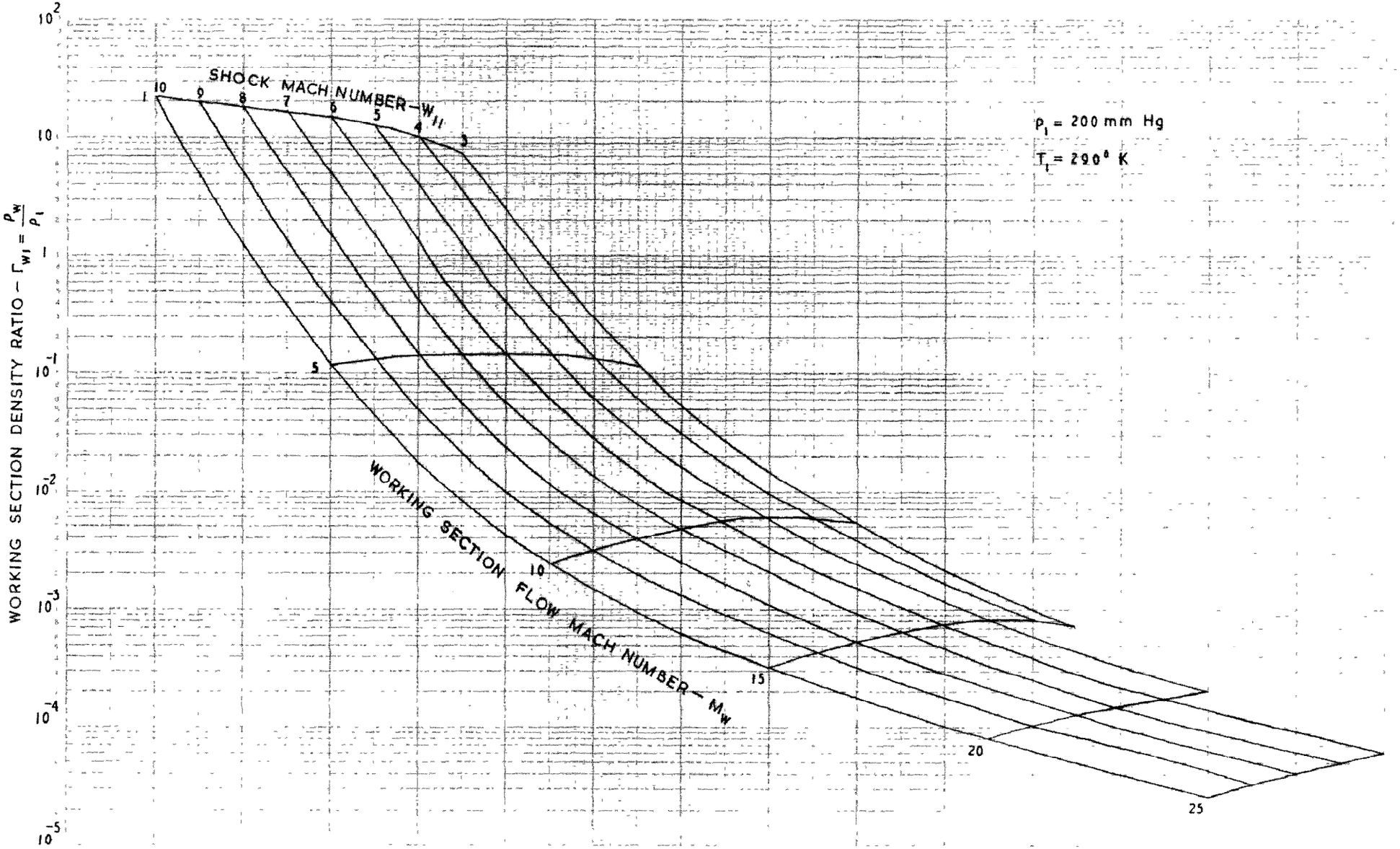

FIG. 7 (b)

FIG. 7 (b) WORKING-SECTION STATIC DENSITY

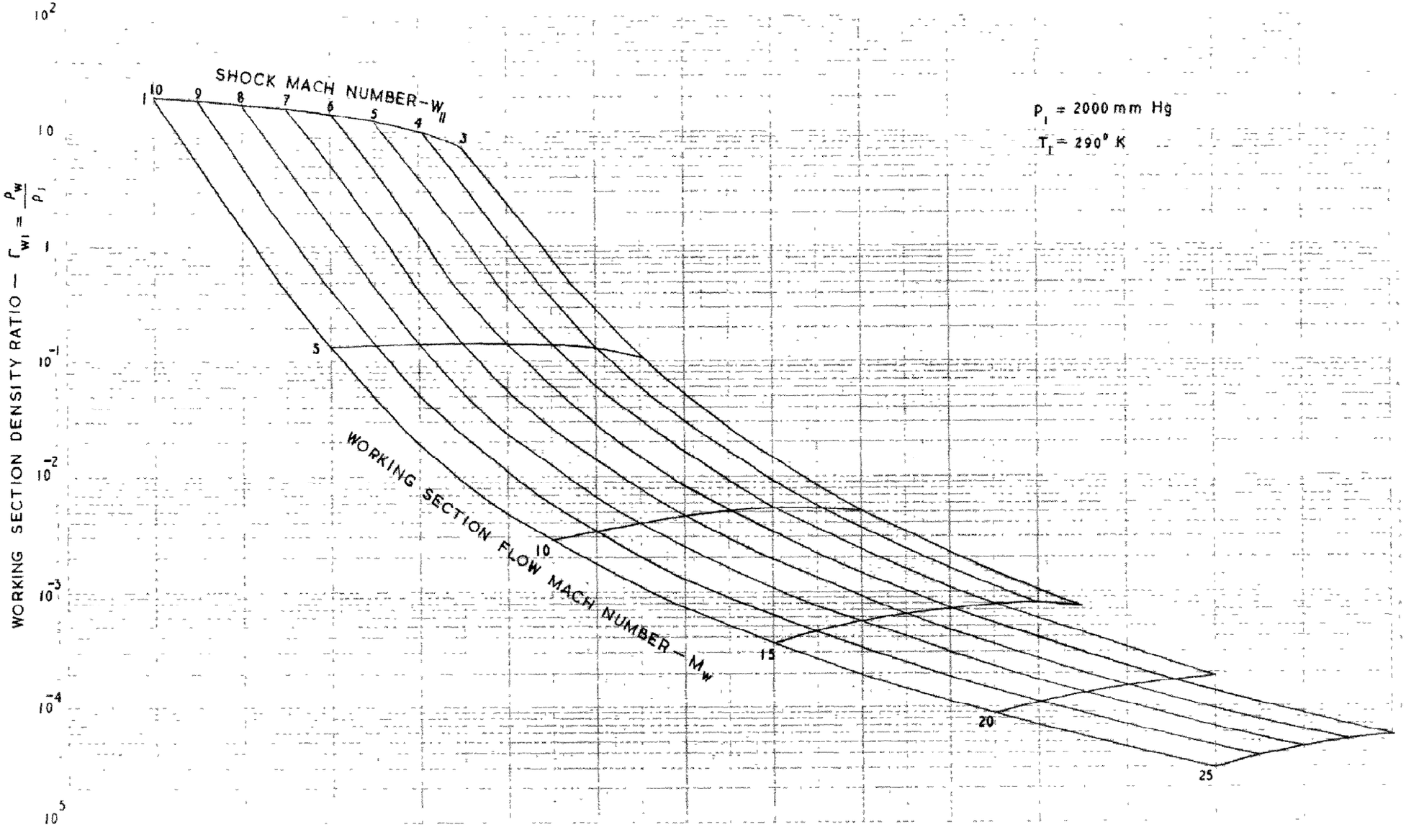

FIG. 7 (c)

FIG. 7 (c) WORKING-SECTION STATIC DENSITY

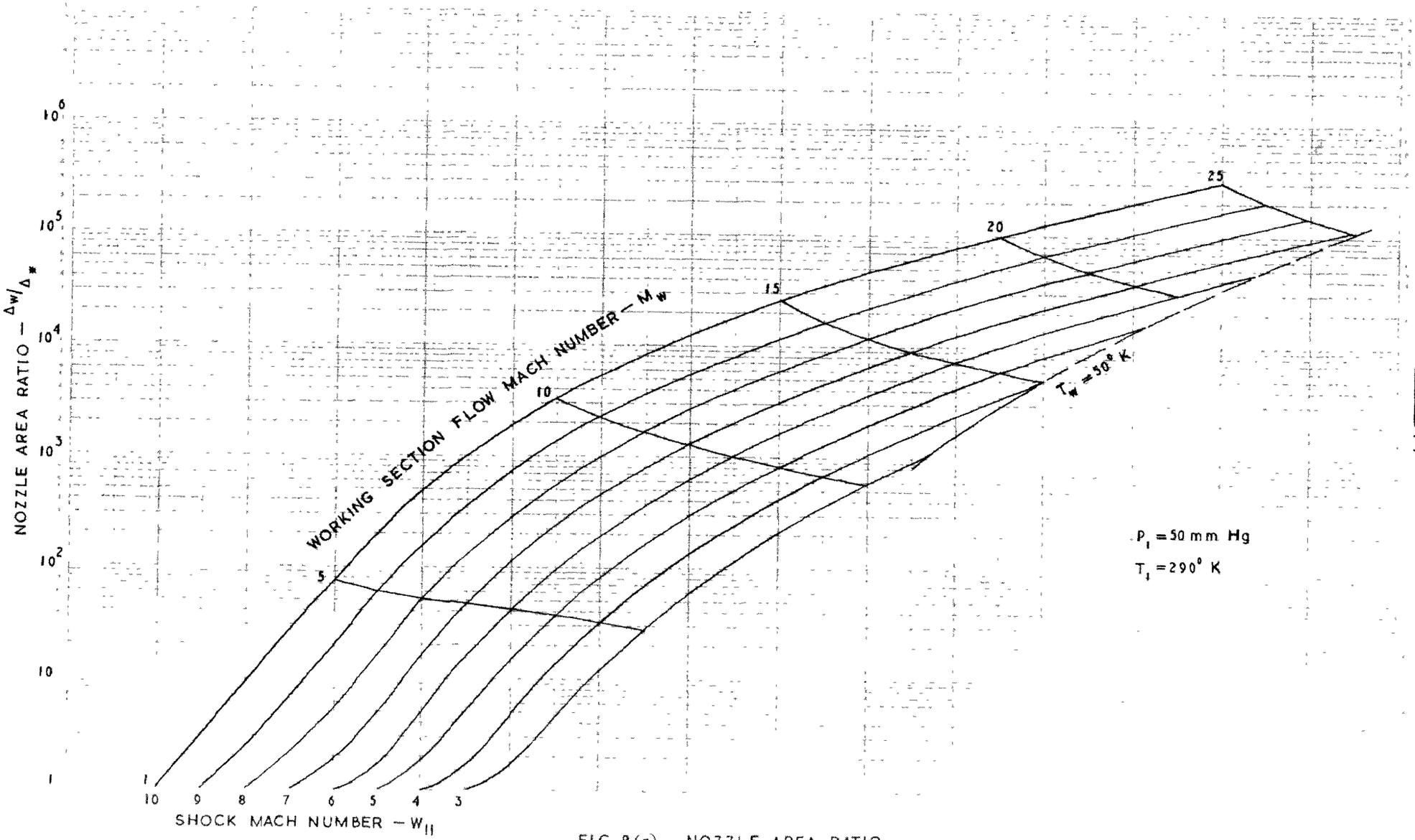

FIG. 8(a) NOZZLE AREA RATIO

FIG. 8 (a)

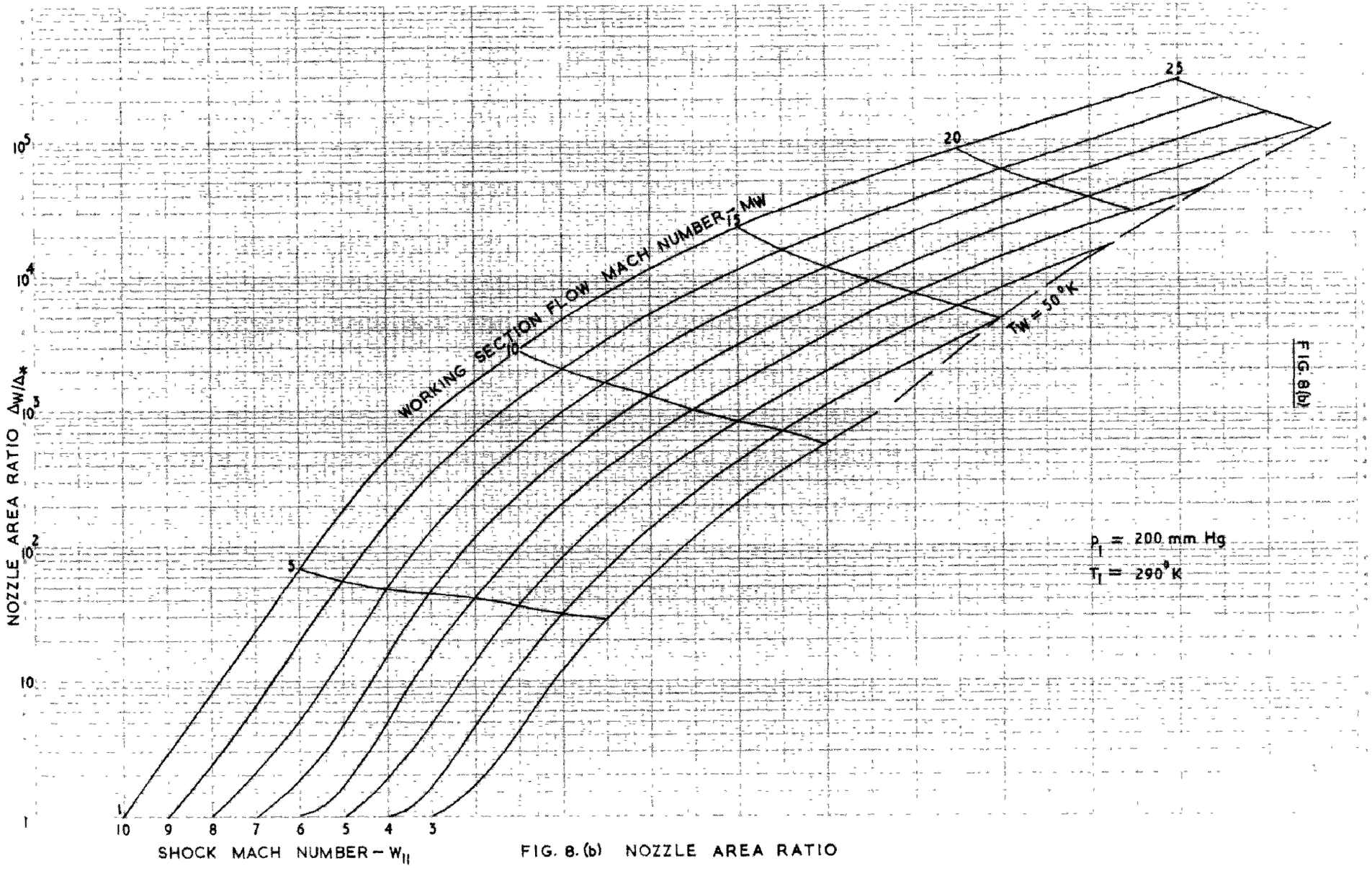

FIG. 8. (b) NOZZLE AREA RATIO

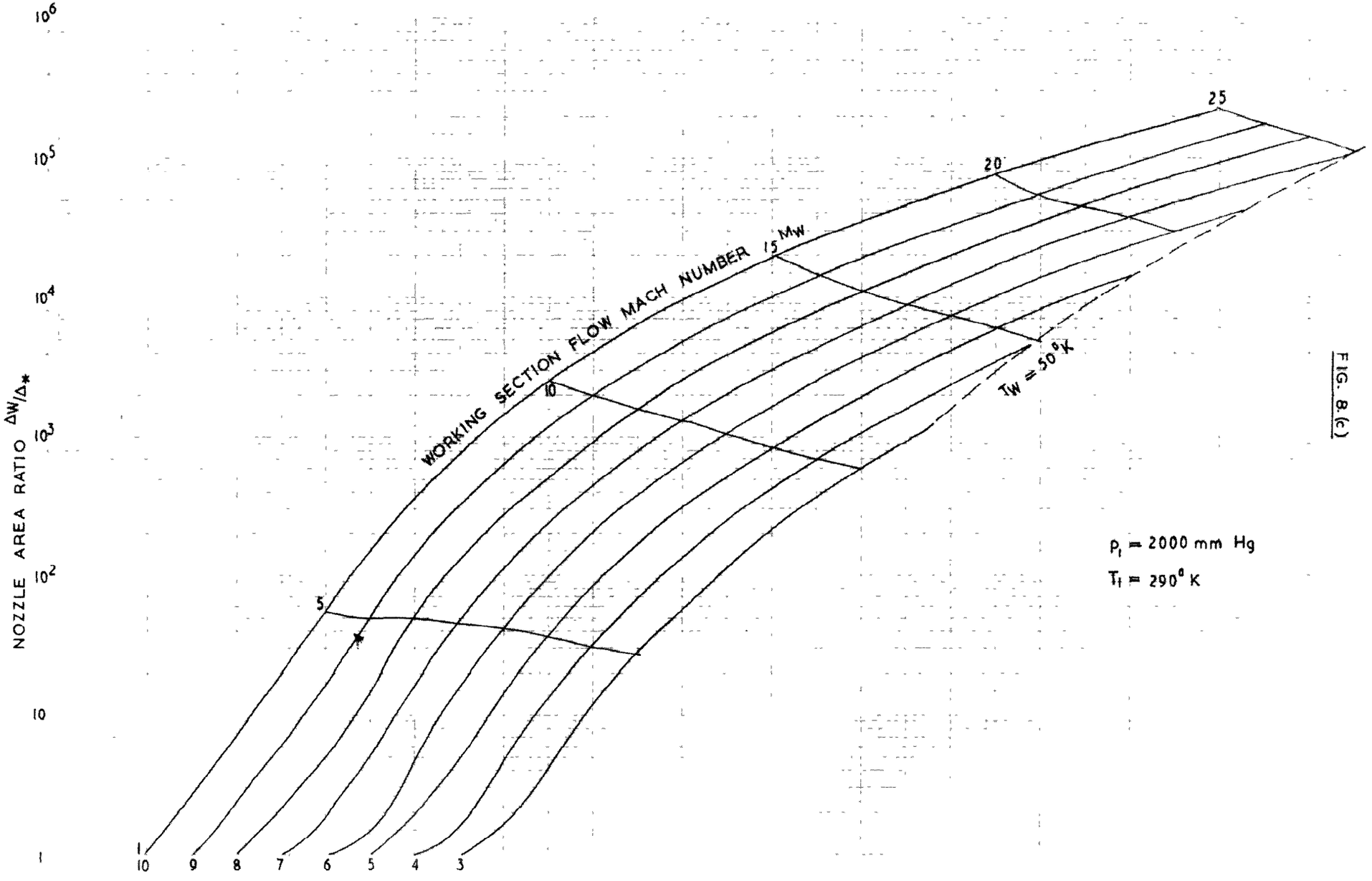

FIG. 8. (c) NOZZLE AREA RATIO

FIG. 8 (c)

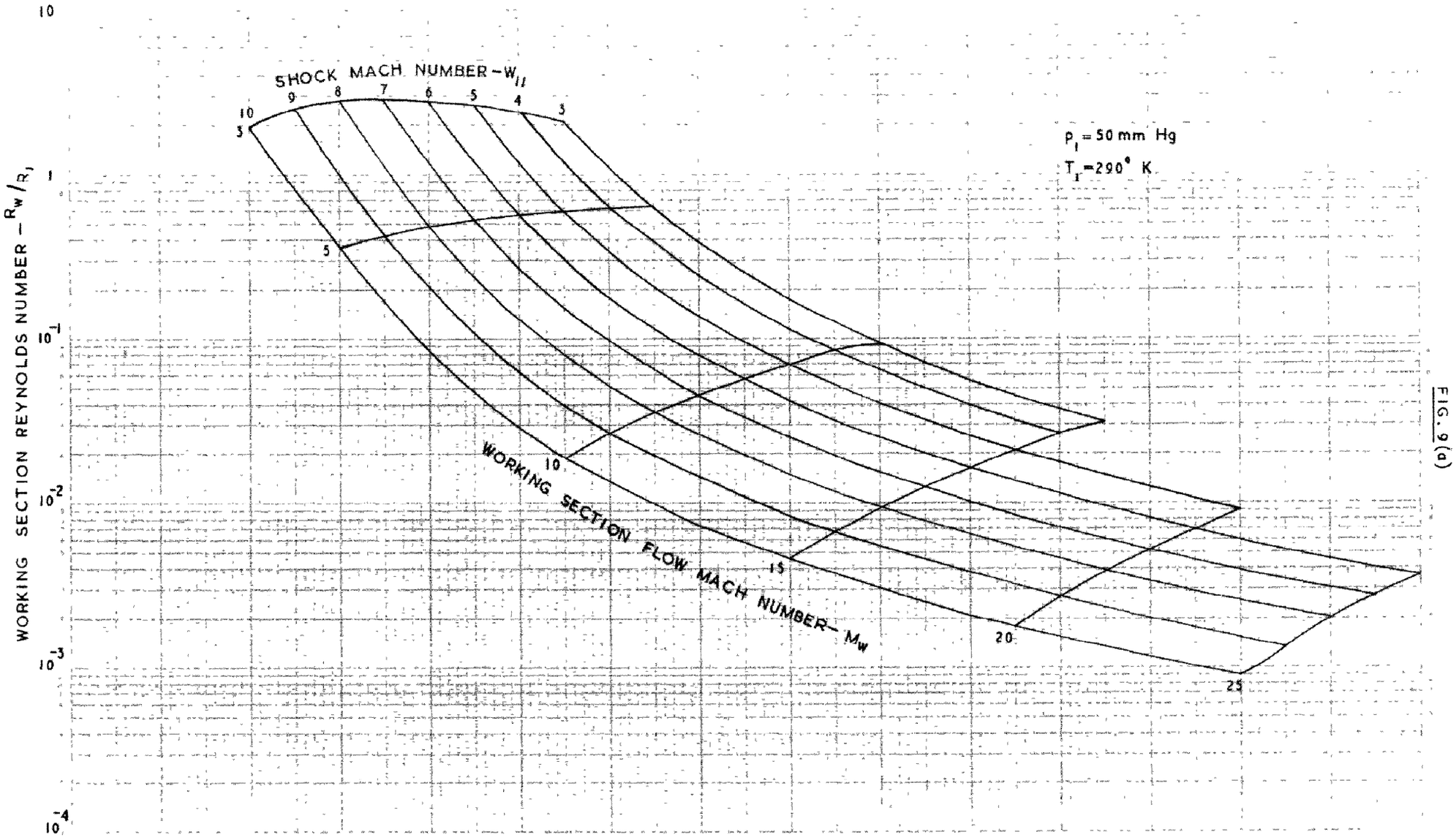

FIG. 9(a)

FIG. 9(a) WORKING-SECTION REYNOLDS NUMBER

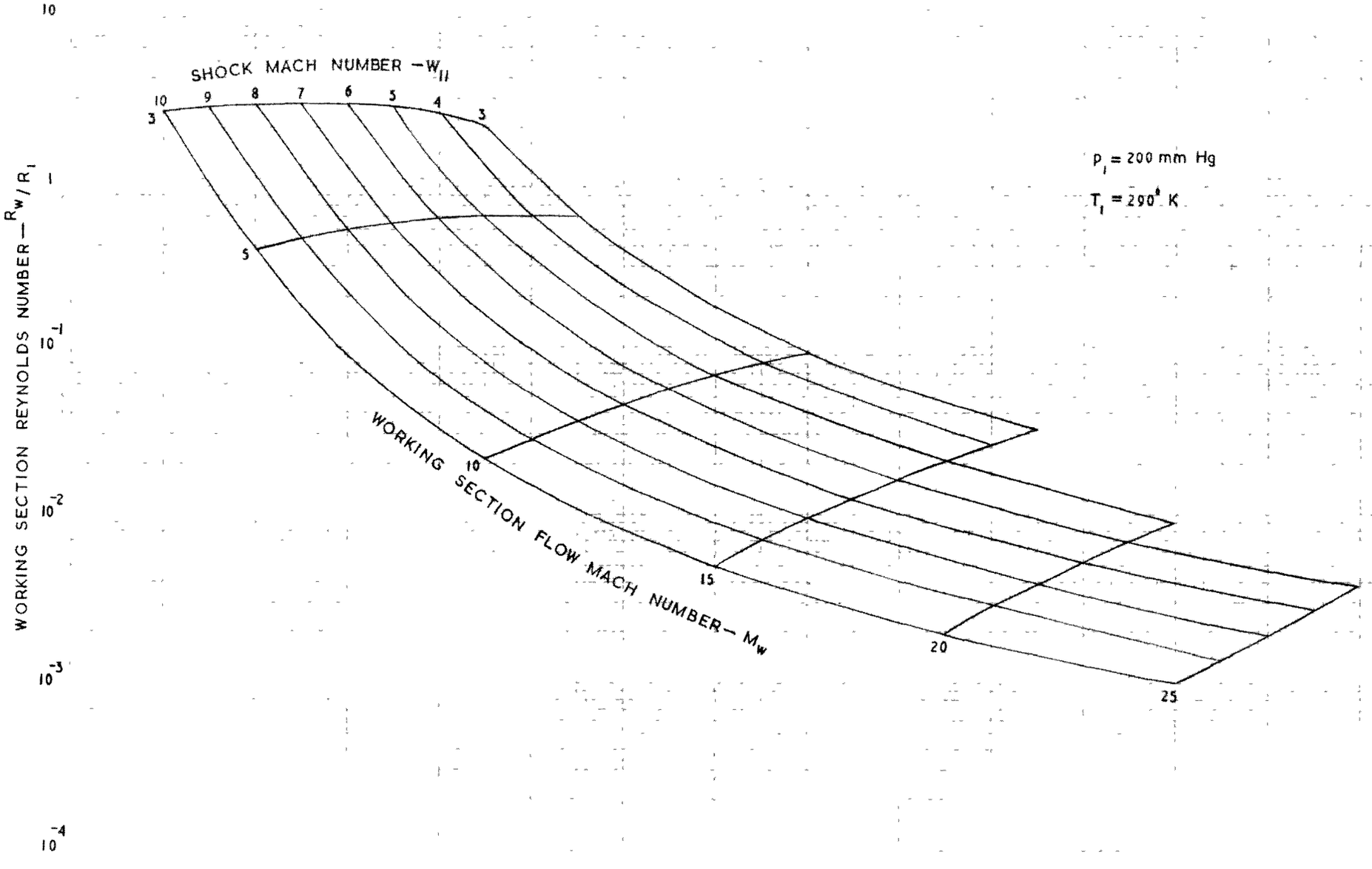

FIG. 9 (b)

FIG. 9 (b) WORKING-SECTION REYNOLDS NUMBER

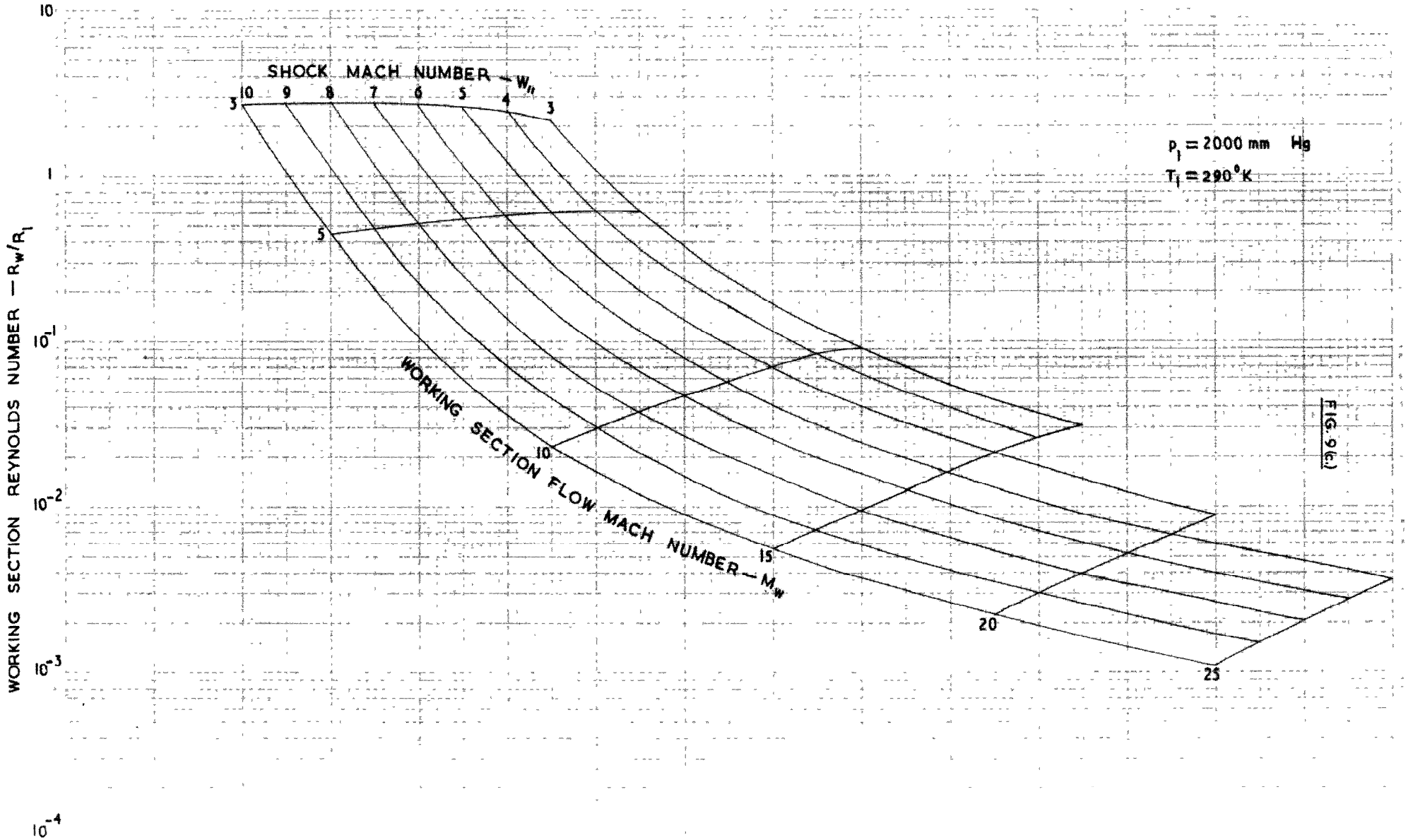

FIG. 9 (c) WORKING – SECTION REYNOLDS NUMBER

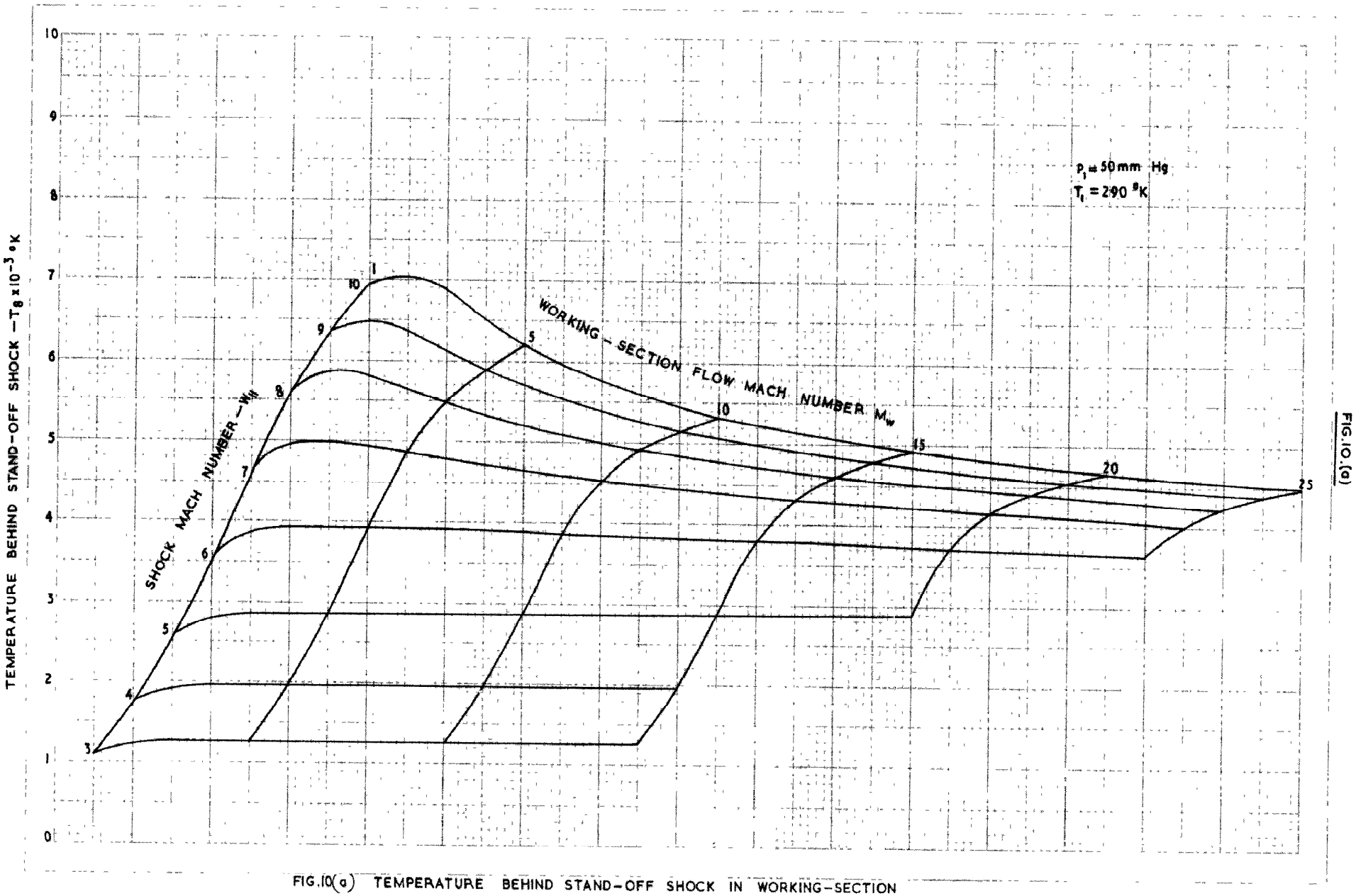

FIG.10(a) TEMPERATURE BEHIND STAND-OFF SHOCK IN WORKING-SECTION

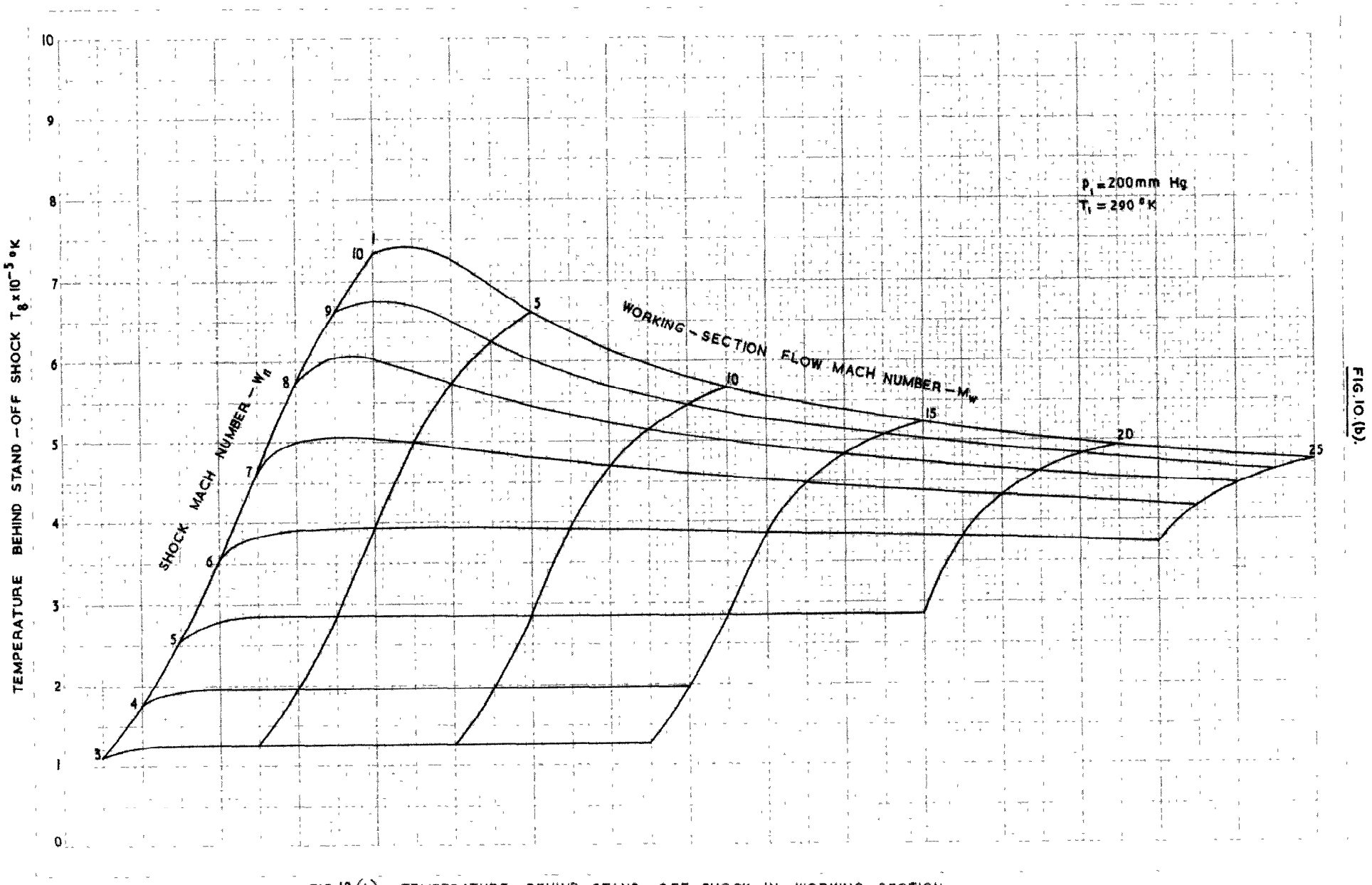

FIG. 10.(b).

FIG.10.(b) TEMPERATURE BEHIND STAND-OFF SHOCK IN WORKING-SECTION.

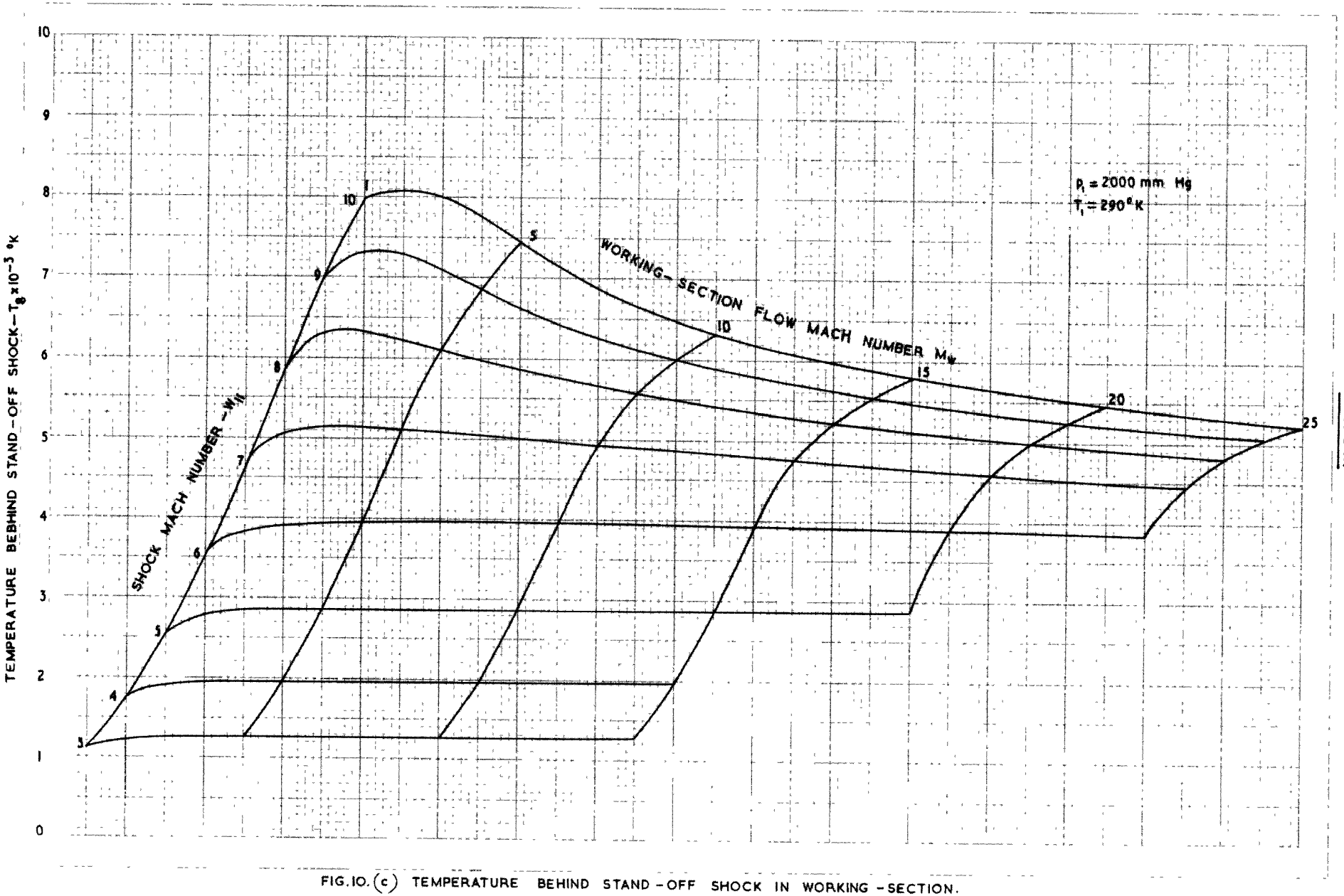

FIG. 10. (c) TEMPERATURE BEHIND STAND-OFF SHOCK IN WORKING-SECTION.

FIG. 10(c).

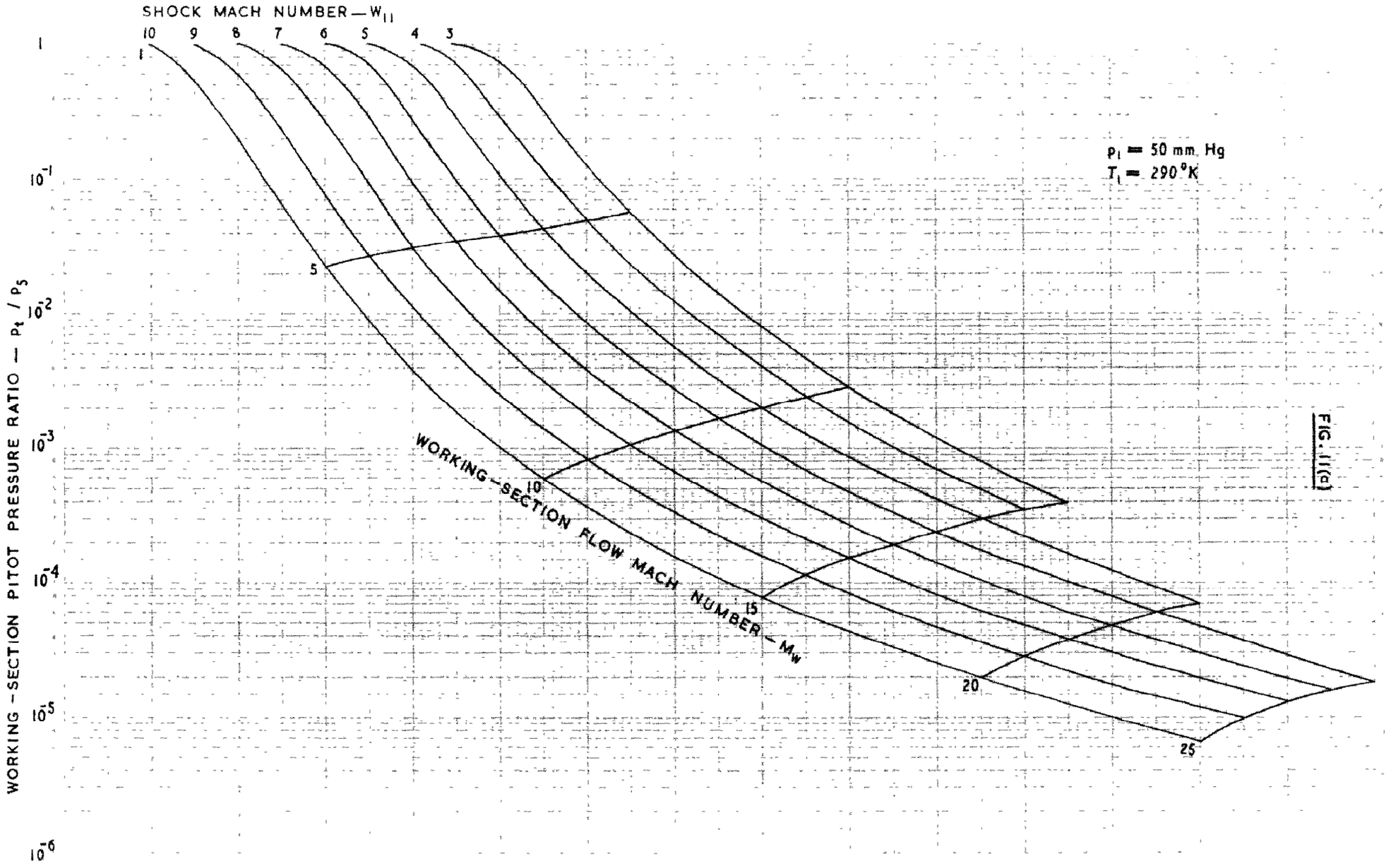

FIG. 11. (a) WORKING - SECTION PITOT PRESSURE

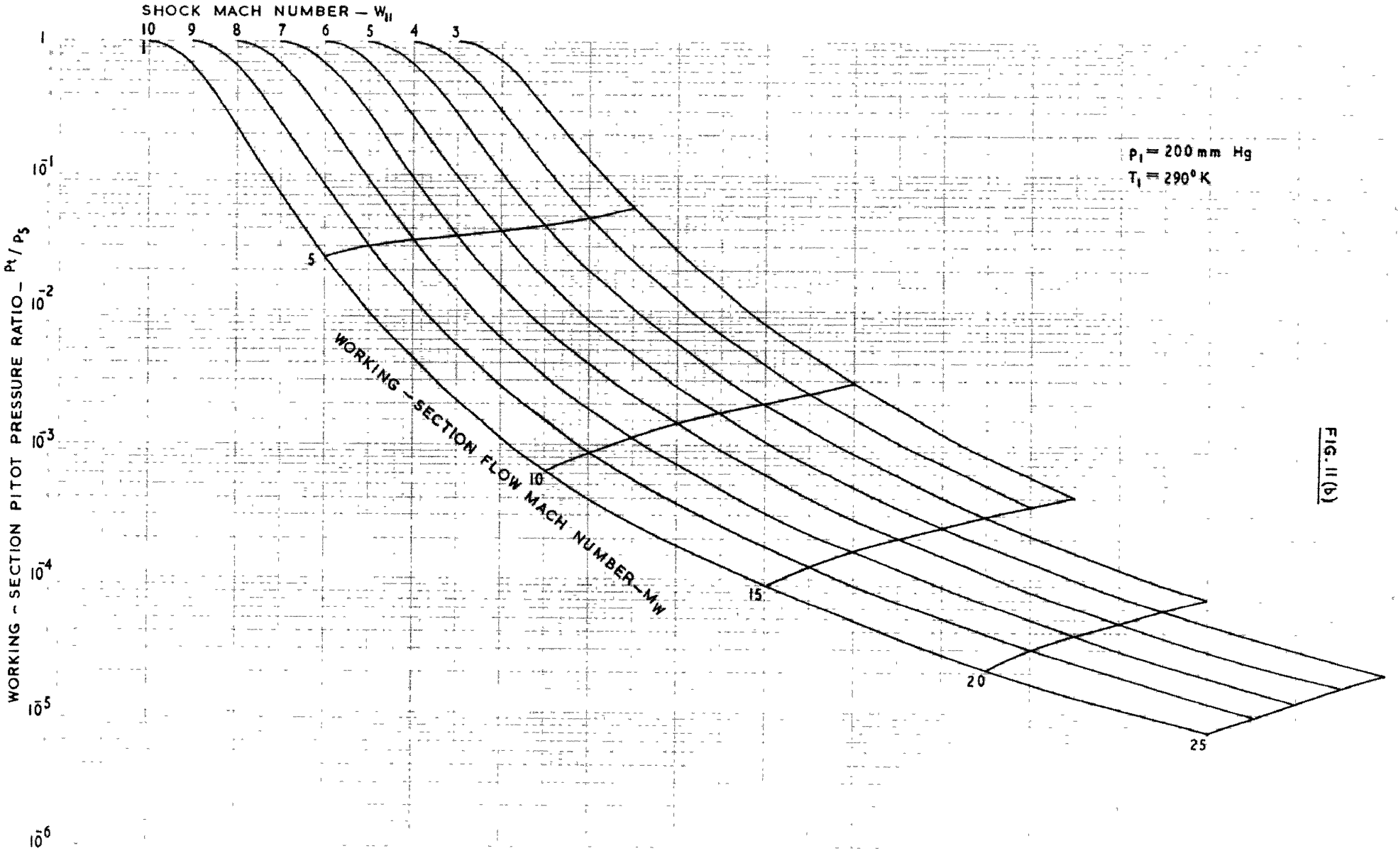

FIG. 11 (b) WORKING – SECTION PITOT PRESSURE

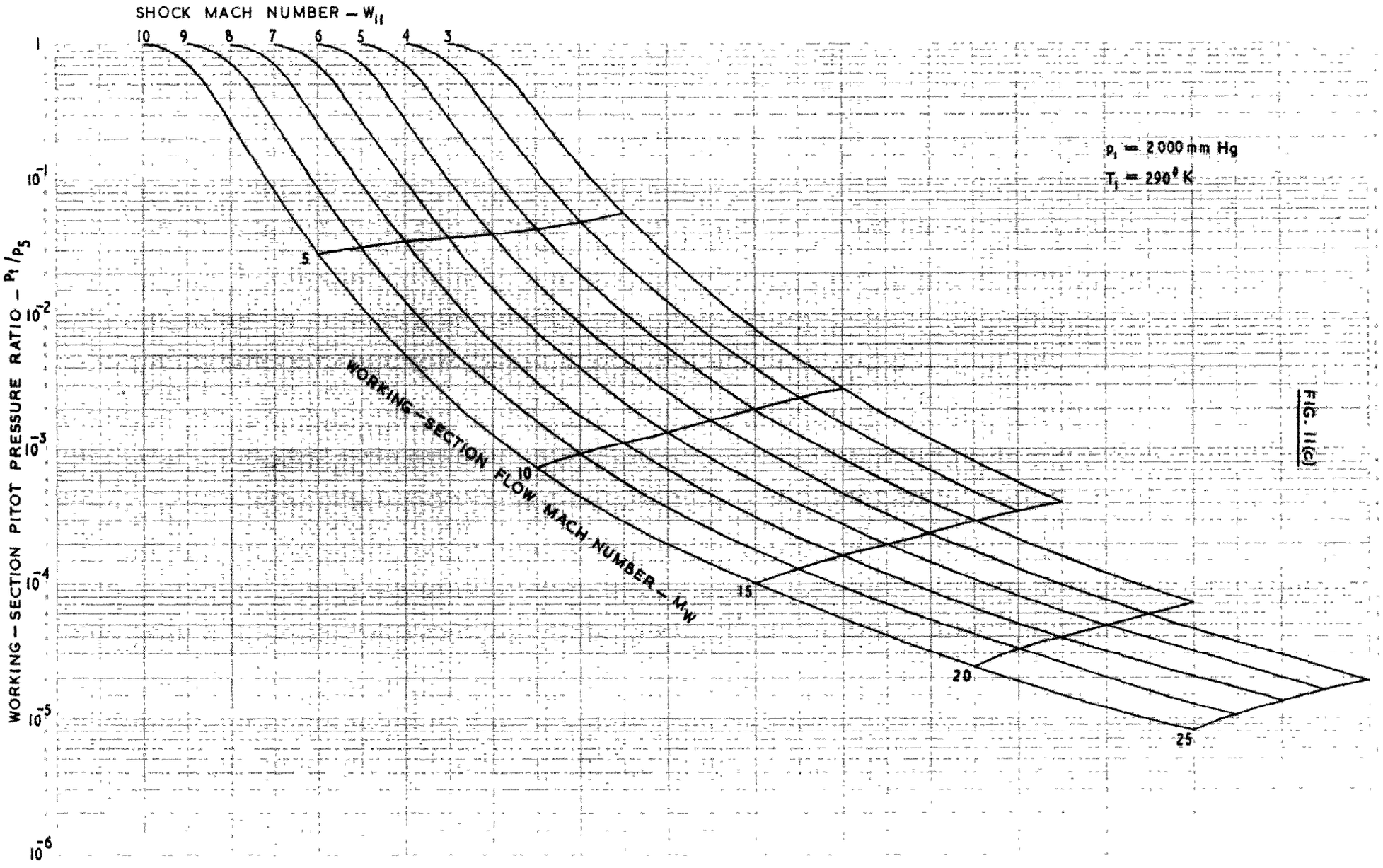

FIG 11 (c) WORKING – SECTION PITOT PRESSURE

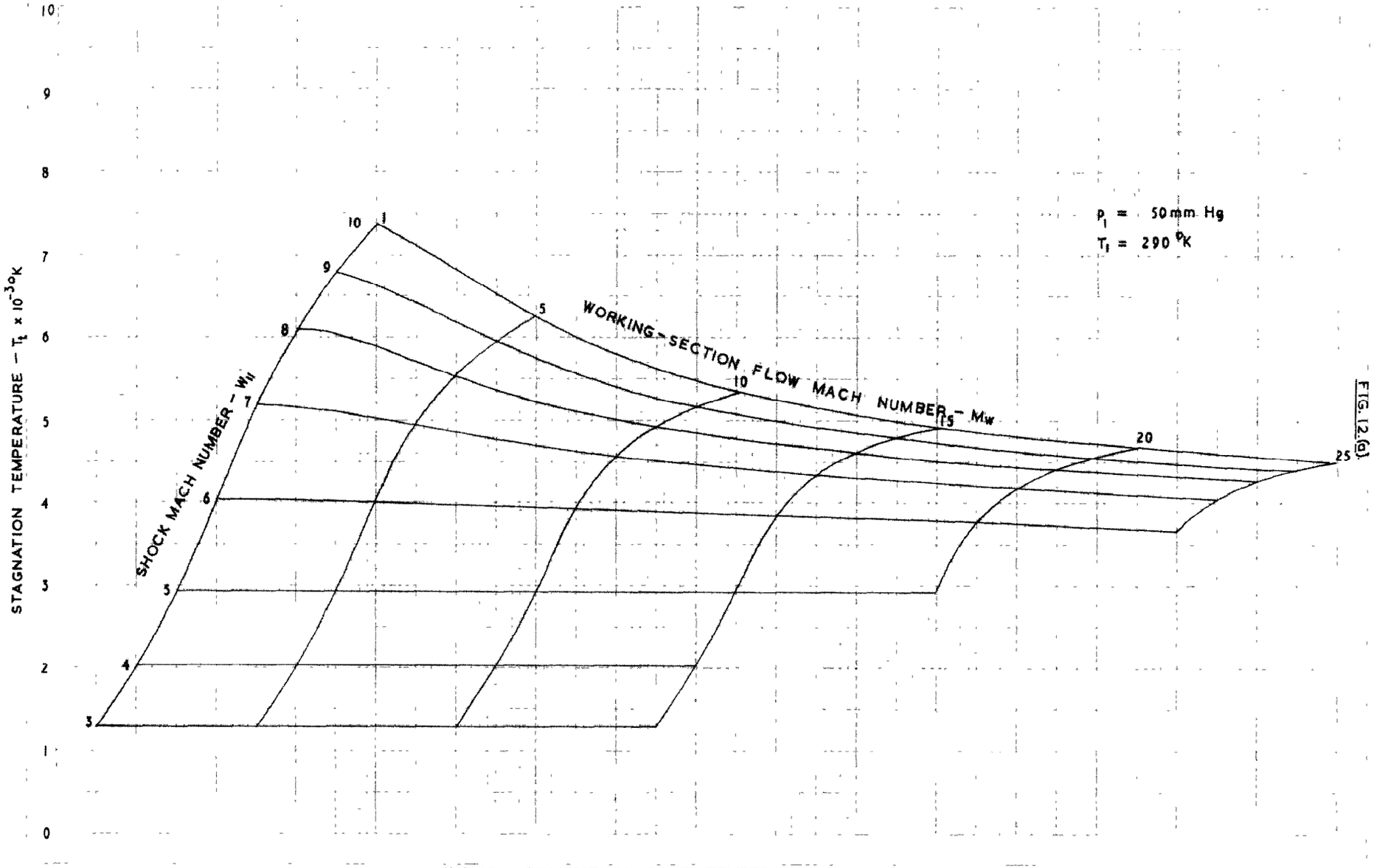

FIG. 12 (a) STAGNATION POINT TEMPERATURE IN WORKING-SECTION

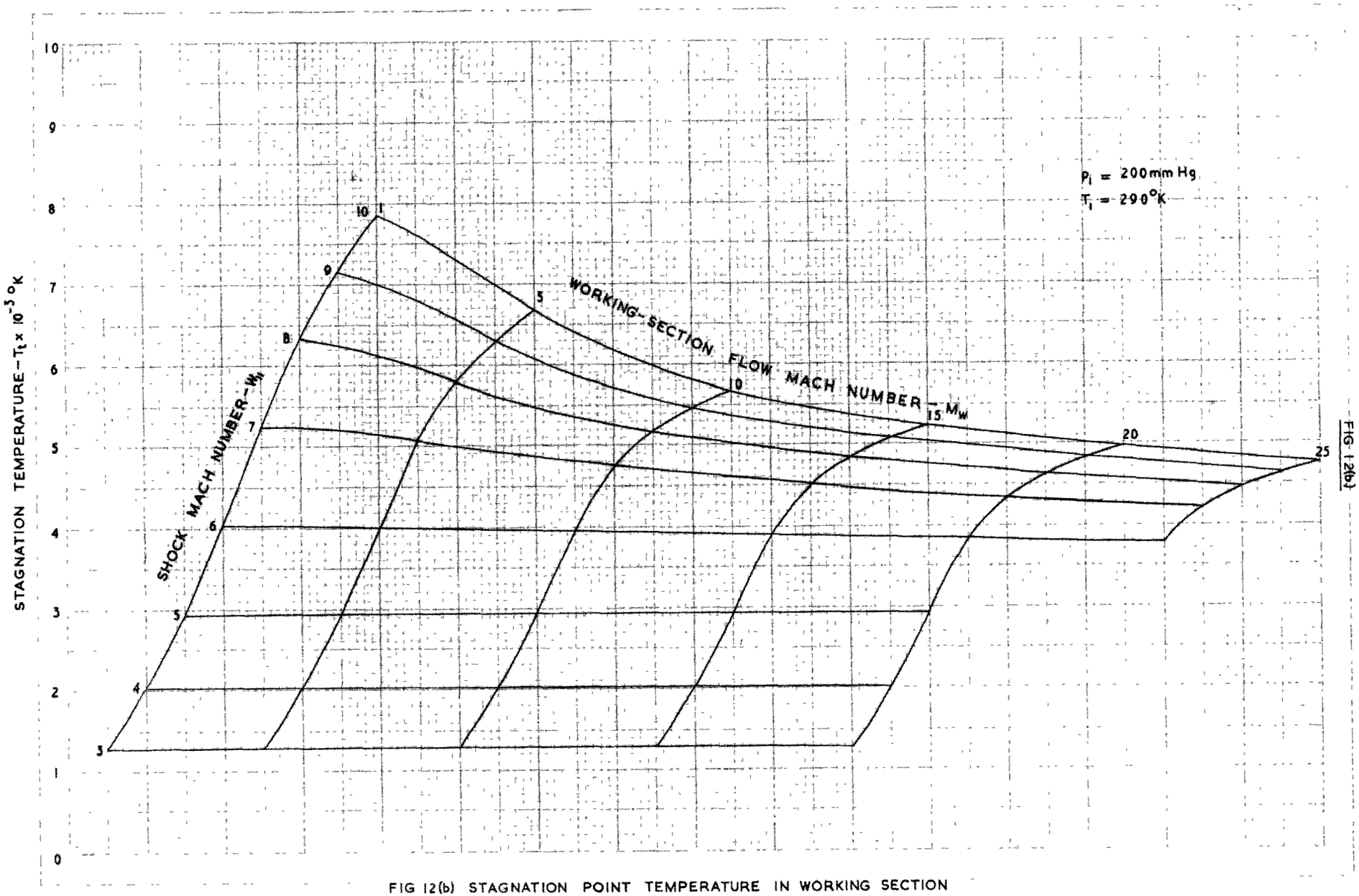

FIG 12(b) STAGNATION POINT TEMPERATURE IN WORKING SECTION

FIG 12(b)

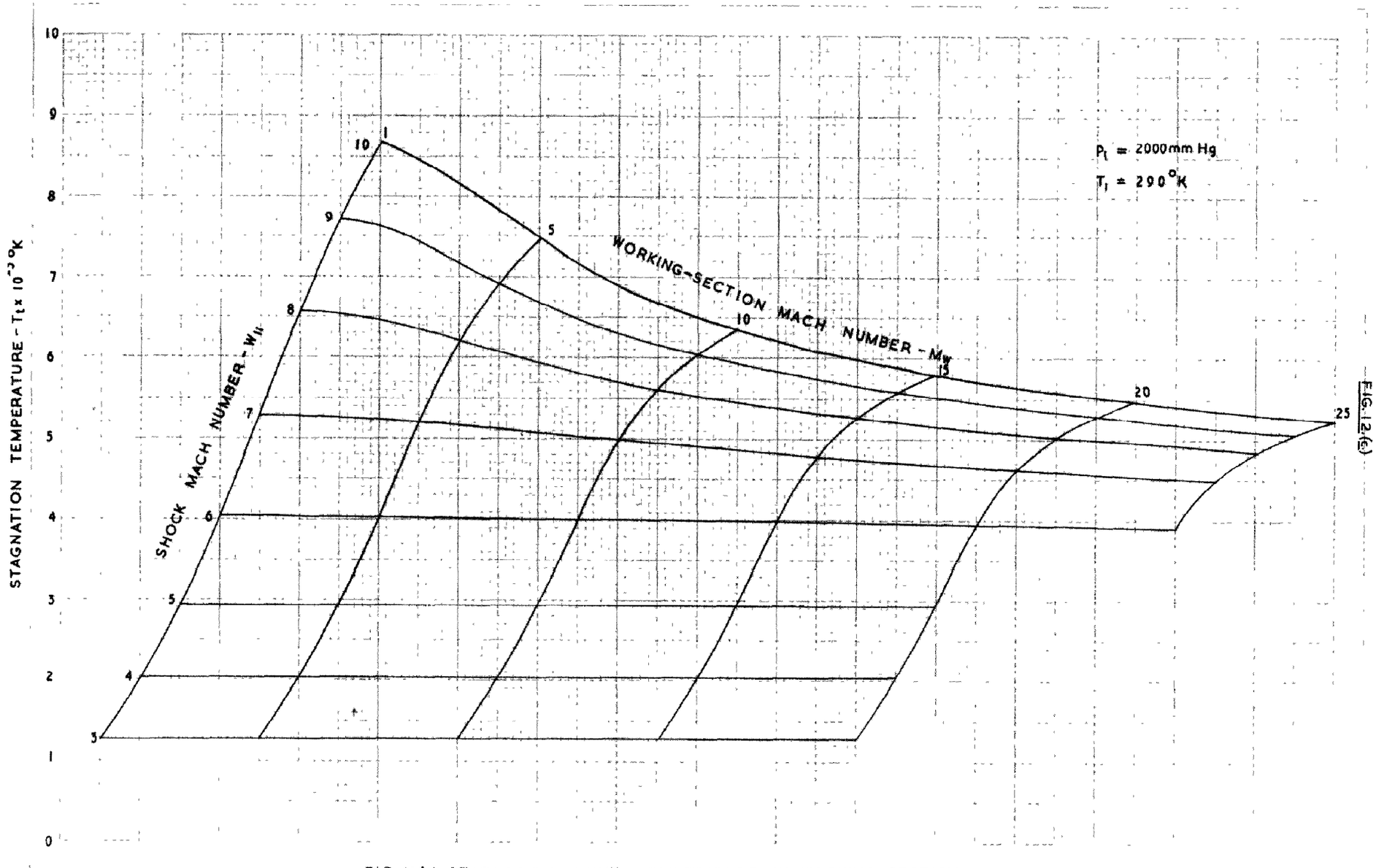

FIG. 12(c) STAGNATION POINT TEMPERATURE IN WORKING-SECTION

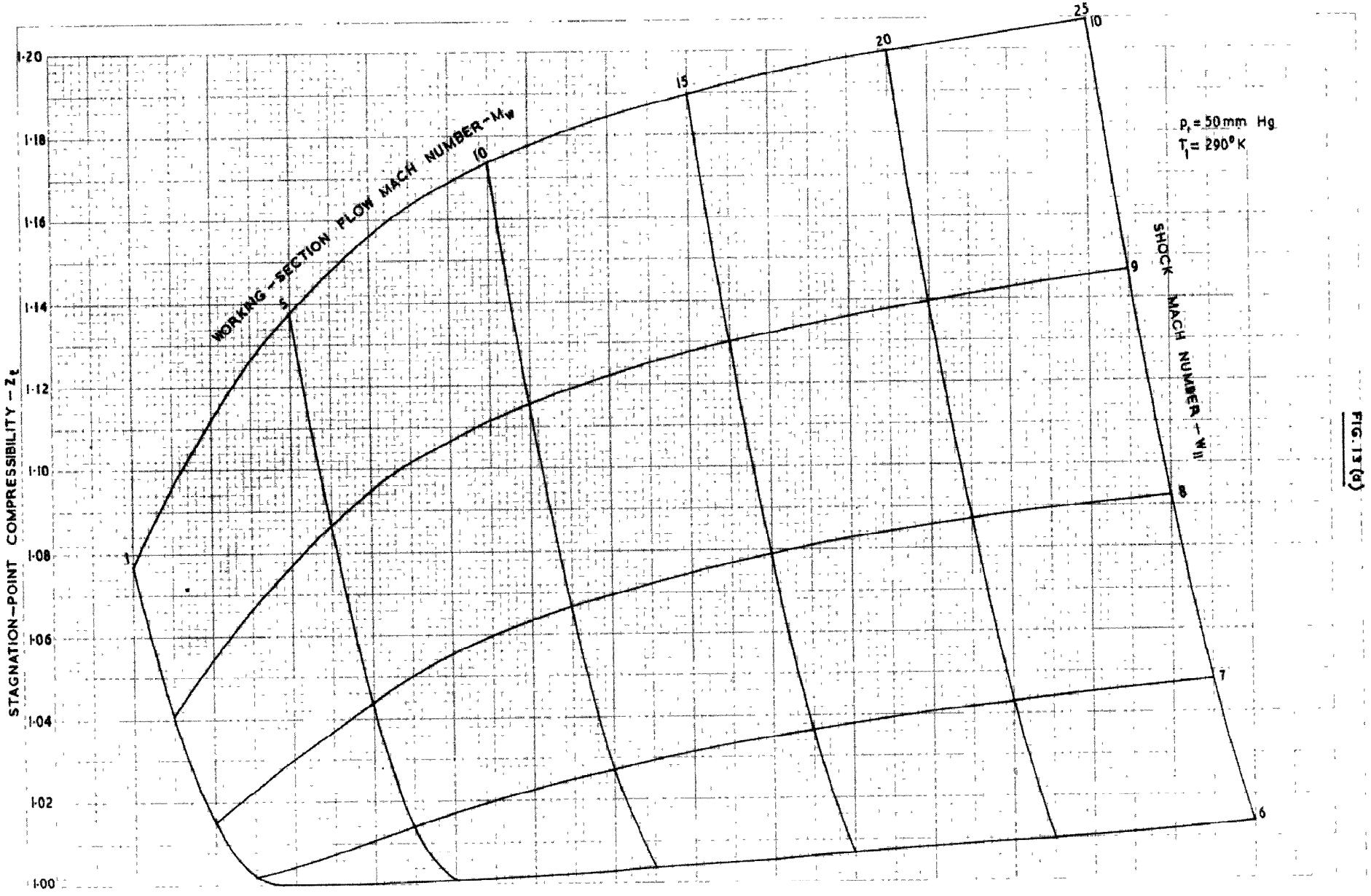

FIG. 13(a)

FIG.13(a) STAGNATION-POINT COMPRESSIBILITY IN WORKING-SECTION.

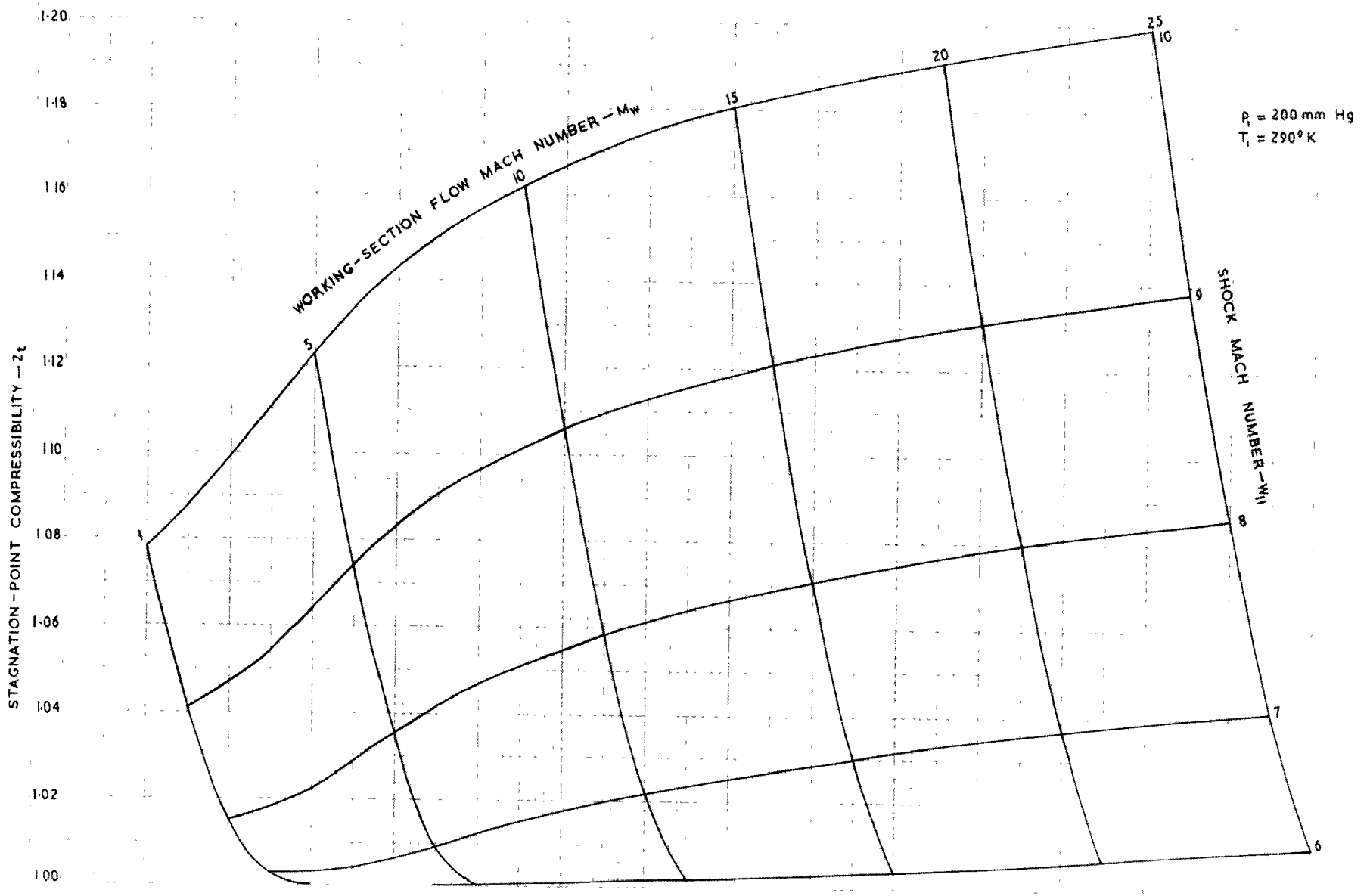

FIG 13 (b) STAGNATION-POINT COMPRESSIBILITY IN WORKING-SECTION

FIG 13 (b)

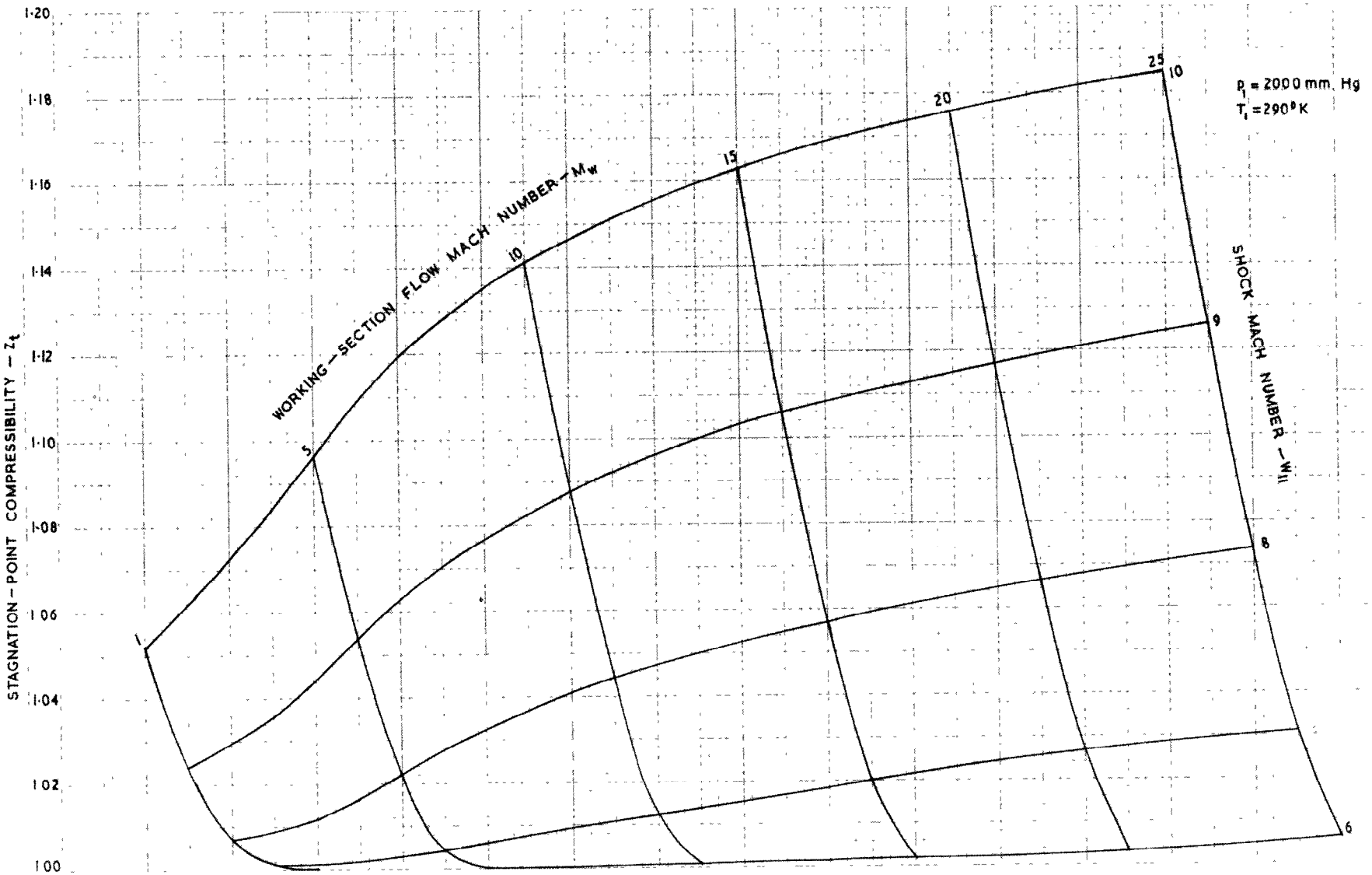

FIG.13 (c) STAGNATION – POINT COMPRESSIBILITY IN WORKING – SECTION

FIG.13 (c)

A.R.C. C.P. No.633
September, 1961
Bernstein, L.

EQUILIBRIUM REAL-GAS PERFORMANCE CHARTS FOR A HYPERSONIC SHOCK-TUBE WIND-TUNNEL EMPLOYING NITROGEN

Charts are presented covering a wide range of reflected-shock wind-tunnel operating conditions, using nitrogen as the working gas. A statistical-mechanical model of the gas is assumed which takes account of molecular vibration, electronic excitation and dissociation. The gas is assumed to be constantly in equilibrium - that is, the reaction rates are taken to be infinitely fast. The equations of motion are solved with the aid of a digital computer, previously reported results[1] for the state of the shock-processed gas in the shock-tube being used.

A.R.C. C.P. No.633
September, 1961
Bernstein, L.

EQUILIBRIUM REAL-GAS PERFORMANCE CHARTS FOR A HYPERSONIC SHOCK-TUBE WIND-TUNNEL EMPLOYING NITROGEN

Charts are presented covering a wide range of reflected-shock wind-tunnel operating conditions, using nitrogen as the working gas. A statistical-mechanical model of the gas is assumed which takes account of molecular vibration, electronic excitation and dissociation. The gas is assumed to be constantly in equilibrium - that is, the reaction rates are taken to be infinitely fast. The equations of motion are solved with the aid of a digital computer, previously reported results[1] for the state of the shock-processed gas in the shock-tube being used.

A.R.C. C.P. No.633
September, 1961
Bernstein, L.

EQUILIBRIUM REAL-GAS PERFORMANCE CHARTS FOR A HYPERSONIC SHOCK-TUBE WIND-TUNNEL EMPLOYING NITROGEN

Charts are presented covering a wide range of reflected-shock wind-tunnel operating conditions, using nitrogen as the working gas. A statistical-mechanical model of the gas is assumed which takes account of molecular vibration, electronic excitation and dissociation. The gas is assumed to be constantly in equilibrium - that is, the reaction rates are taken to be infinitely fast. The equations of motion are solved with the aid of a digital computer, previously reported results[1] for the state of the shock-processed gas in the shock-tube being used.

Printed and published by
HER MAJESTY'S STATIONERY OFFICE

To be purchased from
York House, Kingsway, London, w.c.2
423 Oxford Street, London w.1
13A Castle Street, Edinburgh 2
109 St. Mary Street, Cardiff
39 King Street, Manchester 2
50 Fairfax Street, Bristol 1
35 Smallbrook, Ringway, Birmingham 5
80 Chichester Street, Belfast 1
or through any bookseller

Printed in England

S.O. Code No. 23-9013-33